Revista Brasileira de Geomorfologia

v. 27, nº 2 (2026)

http://dx.doi.org/10.20502/rbg.v27i2.2627

https://rbgeomorfologia.org.br/
ISSN 2236-5664

Research Article

Geomorphological evolution of the Paraguay River fluvial plain in the Corumbá reach, Pantanal, Brazil

Evolução geomorfológica da planície fluvial do rio Paraguai no trecho Corumbá, Pantanal, Brasil

Hudson de Azevedo Macedo[1] José Cândido Stevaux[2] Aguinaldo Silva[1], and Mario Luis Assine[3]

[1] Universidade Federal de Mato Grosso do Sul, Faculdade de Engenharias, Arquitetura e Urbanismo e Geografia, Campo Grande-MS, Brasil. E-mail: hudson.macedo@ufms.br; aguinaldo.silva@ufms.br
ORCID: https://orcid.org/ 0000-0003-1104-7106; https://orcid.org/0000-0002-0630-9768

[2] Universidade Federal de Mato Grosso do Sul, Campus de Três Lagoas, Três Lagoas-MS, Brasil. E-mail: josecstevaux@gmail.com
ORCID: https://orcid.org/0000-0001-6136-2556

[3] Universidade Estadual Paulista, Instituto de Geociências e Ciências Exatas, Rio Claro-SP, Brasil. E-mail: mario.assine@unesp.br
ORCID: https://orcid.org/0000-0002-3097-5832

Received: 09/10/2025; Accepted: 03/06/2026; Published: 28/06/2026

Abstract: The Pantanal wetland, located in the Upper Paraguay River Basin, is the world's largest tropical wetland and a key region for understanding fluvial system responses to Late Quaternary climatic changes. This study investigates the geomorphological evolution of the Paraguay-Corumbá Fluvial Plain (PCFP; approximately 18.3°S to 19.4°S and 57.0°W to 57.8°W) using remote sensing, sedimentological analysis, and OSL dating. We identified three main geomorphological compartments: (1) a floodbasin with topographically elevated channels; (2) an abandoned meander belt; and (3) the active meander belt (floodplain) of the Paraguay River. Sedimentary and chronological data indicate that the floodbasin and its topographically elevated channels developed prior to the Last Glacial Maximum (>23 ka), under conditions of high sediment supply and variable discharge. A meandering system (paleomeander belt) was active during the late Pleistocene to early Holocene (ca. 10–9 ka OSL), with its initial formation possibly occurring earlier under wetter late Pleistocene conditions. A final avulsion event near Castelo Bay around 2–1.5 ka resulted in the current meander belt. These changes reflect primarily variations in hydro-sedimentary dynamics, likely driven by regional climatic shifts during the Late Quaternary. Our results provide new insights into the complex evolution of large tropical floodplains and highlight the role of sediment supply and discharge regimes in controlling fluvial style in the Pantanal.

Keywords: Pantanal wetland; Paraguay River; Fluvial geomorphology; Hydro-sedimentology; Paleoenvironmental changes.

Resumo: O Pantanal, localizado na Bacia do Alto Paraguai, é a maior área úmida tropical do mundo e uma região-chave para compreender as respostas dos sistemas fluviais às mudanças climáticas do Quaternário Tardio. Este estudo investiga a evolução geomorfológica da Planície Aluvial Paraguai-Corumbá (PCFP; aproximadamente 18,3°S a 19,4°S e 57,0°W a 57,8°W) usando sensoriamento remoto, análise sedimentológica e datação por OSL. Foram identificados três compartimentos geomorfológicos principais: (1) uma bacia de inundação com canais topograficamente elevados; (2) um cinturão de meandros abandonado; e (3) o cinturão de meandros ativo do rio Paraguai (planície de inundação). Dados sedimentológicos e cronológicos indicam que a bacia de inundação e seus canais topograficamente elevados desenvolveram-se antes do Último Máximo Glacial (>23 ka), sob condições de alto suprimento sedimentar e descarga variável. Um sistema meandrante (paleomeandro) esteve ativo durante o Pleistoceno tardio até o início do Holoceno (cerca de 10–9 ka OSL), com sua formação inicial possivelmente ocorrendo antes, sob condições mais úmidas do Pleistoceno tardio.. Um evento final de avulsão próximo à Baía do Castelo por volta de 2–1,5 ka resultou no cinturão de meandros atual. Essas mudanças refletem principalmente variações na dinâmica hidrossedimentar, provavelmente impulsionadas por mudanças climáticas regionais durante o Quaternário Tardio. Nossos resultados fornecem novos insights sobre a complexa evolução de grandes planícies de inundação tropicais e destacam o papel do suprimento sedimentar e dos regimes de descarga no controle do estilo fluvial no Pantanal.

Palavras-chave: Pantanal; rio Paraguai; geomorfologia fluvial; hidrossedimentologia; mudanças paleoambientais.

1. Introduction

The Paraguay River is the largest tributary of the Paraná River. Its basin occupies a unique geomorphological position, collecting water and sediments from both the Brazilian Central Plateau and the eastern Andes. This position gives it a leading role in the transfer of sediment and biological diversity to the Río de la Plata Basin (Neiff, 2001; Junk et al., 2006). The total area of the Paraguay River Basin is approximately 1 million km², encompassing parts of Brazil, Bolivia, Paraguay, and Argentina (Rebouças et al., 2002; ANA/GEF/PNUMA/OEA, 2003). The river is commonly divided into four segments: the Higher, Upper, Middle, and Lower Paraguay (Almeida, 1945).

In the Upper Paraguay River Basin (UPRB) includes the Pantanal – the largest wetlands on the planet (Alho et al., 1988; Junk et al., 2006; Por, 1995). It is a wide complex of periodically flooded fluvial plains, with the Paraguay River being the trunk river. At the Pantanal watershed outlet, the Paraguay River has an average discharge rate of 2300 m³/s. The Pantanal, which is widely recognized for its biological resources, is also an immense geomorphological system composed of several depositional systems (Assine et al., 2015a; Stevaux et al., 2020).

The Pantanal is a very complex hydrogeomorphological system with a peculiar hydrological regime that controls the functioning of depositional environments. The areas closest to the sedimentary source are mostly composed of river fans (Assine et al., 2005; Corradini, 2011; Facincani et al., 2006; Pupim, 2014; Zani, 2008; Zani et al., 2009; Zani et al. 2012) which retain approximately 90% of the sediment that enters the Pantanal (Assine et al., 2015a). Located among the river fans are the interfan plains, sedimentary bypass regions that transfer sediment to the Paraguay River.

The main geomorphological studies in the Pantanal involved the Paraguay River fluvial plain (Macedo et al., 2014; Kuerten, 2010; Silva, 2010; Assine and Silva, 2009; Souza, 2004), fluvial megafans (Meira et al., 2019; Pupim, 2014; Merino et al., 2013; Zani et al., 2012; Corradini, 2011; Zani et al., 2009; Zani, 2008; Facincani et al. 2006; Assine, 2005; Assine et al., 2014; Kuerten and Stevaux, 2021), and interfan plains (Merino, 2016; Mendes, 2014; Pupim et al., 2014; and Mendes and Assine, 2013). These studies made important progress in the research carried out in the Pantanal as they raised many questions regarding hydro-geomorphological models of distributary and meandering river systems, channel styles, fluvial incision, avulsion, responses of river systems to climate change, and paleohydrology. Despite the important contribution and relevance of studies carried out on the Paraguay River plain, few of them have focused on understanding the responses of fluvial systems to climate changes that occurred in the late Quaternary (e.g. Kuerten, 2010; Kuerten et al., 2013; Silva, 2010; and Macedo et al., 2014).

In the Pantanal, the Paraguay River plain is divided into eight fluvial plains according to hydrological and geomorphological characteristics (Stevaux et al., 2020) and the present study focused on one of them: the Paraguay-Corumbá Fluvial Plain – PCFP (Figure 1). The objectives of this study were to characterize the sedimentology of the PCFP landforms; recognize paleo-hydrological changes that have occurred in the area; and propose an evolutionary model of the depositional system of the PCFP during the Quaternary based on absolute dating.

2. Studied area in the Pantanal context

The study area comprises the floodplain of the Paraguay River in the Corumbá reach, hereafter referred to as the Paraguay-Corumbá Fluvial Plain (PCFP). The term floodplain is preferred as it is more specific, denoting the flat area adjacent to the channel, constructed by alluvial sediments under the current hydrological regime, and subject to periodic flooding (e.g., Lewin and Ashworth, 2014; Fryirs and Brierley, 2013).

The study area is located in the Pantanal sedimentary basin in the UPRB (Figure 1). The basin is superimposed on the Precambrian crystalline rocks of the Amazonian Craton (Del'arco et al., 1982) and Phanerozoic sedimentary rocks. The basin deposits are represented by colluvial and alluvial deposits of the Xaraiés and Pantanal formations. The Pantanal Formation is composed by semi-consolidated to unconsolidated sand, silty-clay, sandy-clay, and sandy-gravel (Del´arco et al., 1982).

The Pantanal is a tectonically active basin and its origin has been associated with the Andean foreland system (Horton and Decelles, 1997; Ussami et al., 1999; Chase et al., 2009). This basin is characterized by several fault blocks forming a N-S elongated depression filled with 500 m of Quaternary sediments (Assine, 2003; Assine and Soares, 2004; Assine et al., 2015c; Paranhos Filho et al., 2013). The elevations of the Pantanal range between 80 and 190 m above sea level, characterizing a depressed region surrounded by the highlands of Maracaju-Campo Grande and Taquari-Itiquira (East), Guimarães and Parecis (North) highlands, Urucum-Amolar (West) and Bodoquena (South) (Assine, 2003).

The trunk system is composed of floodplain segments with distinct hydrosedimentary characteristics, in which the Paraguay River´s water can be confined in a relatively narrow valley or spread over relatively wide areas (Stevaux et al., 2020). The fluvial plains of the trunk system comprise five distinct compartments defined according their morphology (Assine et al., 2015a) and hydrological functioning (Stevaux et al., 2020) (Figure 1).

The Paraguay River flows in a meander belt carved into the sediments of an older, wider valley, which preserves evidence of paleohydrological changes (Macedo et al., 2014). This valley is occupied by the extensive Paraguay-Corumbá Fluvial Plain (PCFP), composed of Holocene and Pleistocene (Pantanal Formation) deposits (Del'arco et al., 1982). The floodplain is constrained by higher residual reliefs, including plateaus and flat surfaces underlain by Precambrian crystalline rocks.

Several landforms comprise the PCFP, which is dominated by meander belts and floodbasins with numerous small lakes, and morphologies inherited from hydro-sedimentary conditions different from the current ones (Macedo et al., 2014). Although still poorly studied, the PCFP is the largest floodplain segment in the Pantanal trunk river, with an average width of 27 km and 125 in length (Assine et al., 2015b). The plain is located in the central portion of the Pantanal (Figure 1), and between 65 and 70 % of the water draining through the Pantanal passes through this region of the Paraguay River (Assine et al., 2015b). This wide fluvial plain narrows at its end at the Miranda River confluence (Figure 1), generating a bottleneck configuration causing an important disturbance in the river hydrological regime (Macedo et al., 2019; Stevaux et al., 2020).

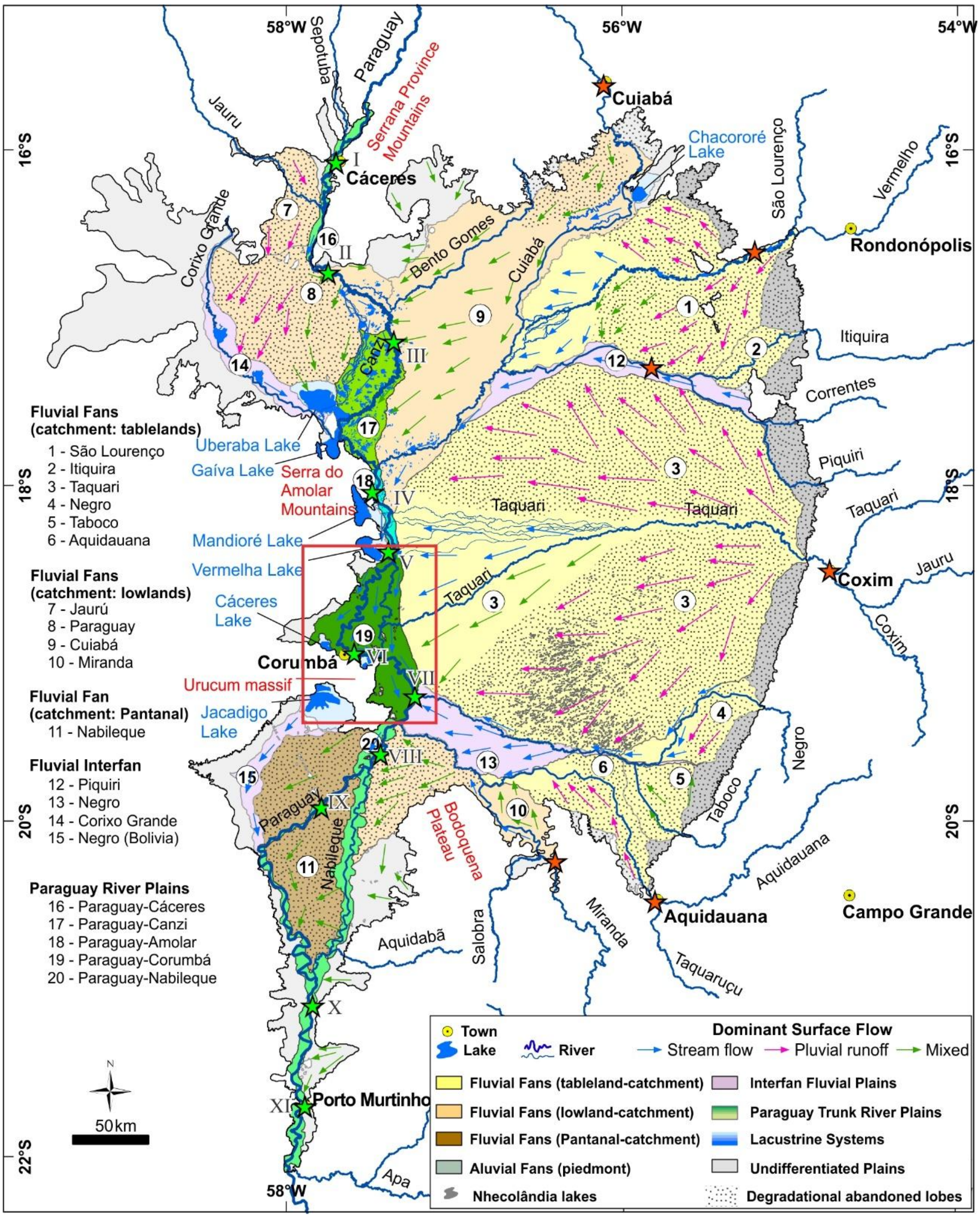

Figure 1. Pantanal morphological map. Location of the studied area in red rectangle (Mod. Assine et al., 2015a). The green stars are gauge stations at the Paraguay River: I) Cáceres; II); Descalvados; III) Porto Conceição; IV) Amolar); V) San Francisco; VI) Ladário; VII) Porto da Manga; VIII) Porto Esperança; IX) Forte Coimbra; X) Barranco Branco; XI) Porto Murtinho. Red stars are gauge stations in the tributary rivers. Coordinates in the WGS-84 datum

To understand the geomorphology of the Paraguay-Corumbá Fluvial Plain, it is necessary to understand the concept that the Pantanal is an active sedimentary basin being filled by a large depositional tract dominated by alluvial sedimentation, where the Paraguay River captures water from different river fans (Assine et al., 2005). Unlike a swamp, the Pantanal is an extensive area that experiences prolonged seasonal flooding that extends from January to June but with flooding peaks in different months for each geographical compartment of the plain.

Three large distinct geomorphological units characterize the studied area: 1) Residual Highland (or Plateau) of Urucum-Amolar, 2) the Paraguay River Depression, and 3) fluvial plains (Franco and Pinheiro, 1982; Macedo, 2017). The fluvial plains are composed of fans and river plains. These are delimited by higher relief formed by Precambrian rocks. These relief are composed of the Paraguay River Depression and residual hills that comprise the Urucum-Amolar Highland.

Pantanal climate is classified as tropical wet and dry (Köppen Aw), with average annual temperatures around 25° C. From September to December, temperatures may reach 40º C and beyond. Between May and July, temperatures decrease due to incursions of southern cold fronts. In the UPRB, the annual mean precipitation varies, in the S-N direction, between 800 mm in the Gran Chaco and up to 2000 mm in some northern regions at the highlands (Clarke et al., 2003; Assine et al., 2015a,b; Marengo et al., 2015).

The atmospheric flow within the Intertropical Convergence Zone or Equatorial Convergence Zone (ITCZ) experiences the opposite influences of the patterns of the easterly winds (Balek, 1983). The humid tropical climate is affected by the north-south migration of the ITCZ. Therefore, a typical dry-humid climate is evident in the region, with a marked seasonality in rainfall (Garcia, 1984).

It has been recognized that the South Atlantic Convergence Zone (SACZ) play a significant role in defining the inter-annual variability of rainfall over the Pantanal (Marengo et al., 2021). The inter-annual variability recorded in the time series of river level at the central portion of the Paraguay River, revealed years with annual peaks fluctuating accordingly to rainfall up to the mid 1970´s (Bergier & Resende, 2010). By 1974, the inter-annual amplitude of river level has diminished, which has been attributed to anthropogenic ecohydrological alterations between the Plateau and the Pantanal (Bergier, 2013).

The distribution of annual precipitation is controlled by the South America Summer Monsoon (SASM), leading to heavy convective rains in the austral summer and markedly dry conditions during the winter. A very deep continental low forms over the Chaco region during the austral summer and forces easterly winds over Amazonia to move southward, transporting large amounts of moisture that feed summer convective storms over the subtropical lowlands to latitudes 35° S (Garreaud et al., 2009).

3. Materials and methods

3.1. Geomorphological analysis

We used data from remote sensors Image Landsat 7 ETM +, from the dry season, scene 227/73, November 2003; HCR images, CBERS 2B; SRTM altimetric data with a spatial resolution of 30 m, obtained by TOPODATA interpolation (Macedo et al., 2014), and images from Google Earth and RapidEye.

The optical images and Digital Elevation Model (DEM) were joined and cut according to the limits of the studied area, and the DEM of the area was generated by reducing the altimetry class intervals to emphasize the landforms. The products (colored composition and DEM) were visually analyzed to identify the existing morphologies. First, the areas above the plain, that is, the Urucum-Amolar Highland and the Paraguay River Depression, were delimited followed by the landforms identified in the Paraguay River Plain were delimited.

The criteria for delimiting the compartments were the recognition of the landform's characteristic of each compartment (oxbow lakes, scroll bars, topographically elevated channels, etc.). The limits between fluvial plains and the highest landforms (distal river fans and basement) were defined by the altimetric differences observed in the DEM and by the difference in texture recognized in the ETM+ image. The compartments of the PCFP were delimited by the difference in texture observed in the optical images (RGB composition), and by the height difference recognized in the DEM.

An empirical equation to estimate the bankfull discharge of the Paraguay River was developed by Macedo (2017) based on measurements of channel width and meander wavelength. Discharge measurements of the Paraguay River were made in its upper segment (reach 1 – see item 4.1.3, Figure 2 and table 2). The discharge of the Paraguay River in its upper section can be estimated based on the following expression:

$$y = -0.11056x1 + 0.728813x2 + 1{,}503.904 \quad (1)$$

where y is the average annual flow in $m^3\ s^{-1}$, x1 is the average channel width in meters, and x2 is the meander wavelength in meters (Table 1). Then, this equation was used to estimate paleodischarges from paleochannels of the paleomeander belt (see Supplementary Material F-1).

While the application of empirical hydraulic geometry relationships to paleochannels requires caution due to potential changes in channel geometry and flow regime (Williams, 1988), Equation 1 provides a first-order approximation for comparing paleo and modern hydraulics. The chosen parameters—channel width and meander wavelength—are among the most robust morphometric indicators preserved in the geological record and have been widely used for paleohydrological reconstructions (e.g., Dury, 1965; Ethridge and Schumm, 2007). The use of channel dimensions as a primary proxy for interpreting ancient river systems is well-established in fluvial sedimentology (Gibling, 2006). The regression was developed specifically for the Paraguay River in its upper reaches, which strengthens its application to paleochannels within the same system, assuming broadly similar boundary conditions. The estimated accuracy of ± 8.41 m^3s^{-1} reflects the fit of the regression for the modern river, but the total uncertainty when applied to paleochannels is certainly higher, encompassing factors such as unknown channel depth and bed roughness. Therefore, the paleodischarge estimates presented here should be interpreted as indicative of a general order of magnitude rather than precise values.

Table 1. The Paraguay River morphometry used to estimate average annual flow. The width is an average of the stretch of the meander arch. For section locations, see chapter 7 of Macedo (2017) - Figure 26. For more information on meander wave widths and lengths, see supplementary material F-1.

Section*	Width (x1)	Meander wavelength (x2)	Mean discharge (y)*
34	228	927	1,558.333
33	257	1,143	1,569.693
32	269	1,710	1,521.100
29	318	2,317	1,471.820
28	291	1,958	1,502.450
27	262	2,257	1,443.918
25	208	2,353	1,395.663
Average	261	1,809	1,494.106

*Source: Macedo (2017)

3.2. Geochronology and sedimentology

Eleven cores were obtained by vibro-corer sampling in the PCFP (Figure 6): four in the paleomeander belt, four in the meander belt, and three in the floodbasin. Of these cores, only ten were sampled for dating using the Optically Stimulating Luminescence method – OSL (Table 3; Supplementary Material F-2). Samples were also obtained by auger drilling.

The cores were photographed and described in the laboratory and presented as traditional sedimentary profiles (Supplementary Material F-2). The grain size was determined using visual–tactile analysis. We used the facies code modified from Miall (1978): Fm, massive mud; Sm, massive sand; S/F, sand and mud layer intercalations; and Sm(o) and Fm(o) - massive sand or mud with organic material and/or vegetal fragments. Sites were selected according to the study interest and access conditions (Figure 6). The cores were opened in a dark-room using a red-light lamp to preserve the energy stored in the quartz crystal structure. After being described and analyzed, the cores were collected and dating.

The Optically Stimulated Luminescence (OSL/SAR) technique (Murray and Wintle, 2000; Wintle and Murray, 2006) was applied to quartz grains of 15 samples at the Gamma Spectrometry and Luminescence Laboratory (LEGaL), Institute of Geosciences (IG), University of São Paulo (USP). Sample preparation followed the procedures described by Sawakuchi et al. (2008). The OSL/SAR analyses were performed using an automatic Risø system (Risø National Laboratory).

Dose rate was estimated by gamma spectrometry with HPGe detector in ultralow background shielding in samples collect 10 cm above and below the datting samples. The equivalent doses were determined using the SAR protocol in multigrain quartz aliquots and are listed in the supplementary material (SM2). Optically stimulated luminescence measurements were performed on a Risø TL/OSL DA-20 reader equipped with beta radiation source (SR/Y) with a dose rate of 0.108 Gy^{-1}/s, using 4 mm diameter discs with approximately 100 grains per aliquot.

Preparation of quartz rates involved: 1) wet sieving to acquire the 180-250 μm fraction; 2) H_2O_2 Attack for elimination of organic matter, 10% HCl attack for carbonate elimination; 3) densimetric separation of heavy and light minerals (LMT = 2.85 g/cm^{-3}) and quartz separation (LMT = 2.62 g/cm^{-3}); and 4) HF attack 38% for 40 min to eliminate the outer layer of quartz grains and reduced feldspars. The dose recovery test was made for the P-11 and P-14 samples (eight aliquots, 200° C preheat, 3Gy and 15 Gy doses). The bleaching was done under natural light simulator for 3 to 4 h. The average of the ratio between calculated doses and the administered dose were 1.03 ± 0.01 for the 3 Gy test and 0.98 ± 0.01 for the 15 Gy test. Only aliquots with recycling ratio between 0.9 and 1.1, recovery lower than 5% and a feldspar contamination test using the OSL IR depletion ratio (Duller, 2003) with a ratio between 0.9 and 1.1 were considered to calculate the equivalent dose.

This study employed Optically Stimulated Luminescence (OSL) dating with the primary objective of establishing a chronological framework for the three distinct geomorphological compartments identified in the study area. The Central Age Model (CAM) was used for equivalent dose and age calculation, a model widely considered appropriate for providing a central estimate of the accumulated dose.

Some samples, inherent to dynamic environments like floodplains, exhibited moderate dispersions (overdispersion values up to 39%). These dispersions reflect the complex transport and depositional history of the sediments, including the potential for partial bleaching. It is important to emphasize that, as the multi-grain protocol was used, the application of alternative models, such as the Minimum Age Model (MAM), is not advisable. The MAM was developed for single-grain data, where it is possible to statistically isolate individual poorly-bleached grains (Galbraith et al., 1999). In multi-grain measurements, the luminescence signal from each aliquot represents an average of dozens or hundreds of grains, which dilutes and masks the signature of individual residual doses, making the statistical identification of a "minimum" population unreliable.

We acknowledge that for samples with higher dispersion, the ages calculated by the CAM may incorporate additional uncertainty. However, the focus of this analysis is not on the absolute dating of each individual sample, but on the relative chronological position and the temporal segregation of the geomorphological compartments. The obtained ages, even those with wider error margins, are consistently distinct and do not overlap when their uncertainty intervals (1 sigma) are considered. This clear temporal separation between compartments confirms the robustness of the geomorphological interpretation, which is the core of the proposed discussion.

Therefore, we chose to present and discuss the ages calculated by the CAM, with their respective uncertainties, as representative of the temporal position of each unit. We conclude that further refinement of the OSL data using more complex models is not necessary to meet the central objective of this study, as the established chronological trend is unambiguous and sufficiently robust to support our conclusions on landscape evolution.

4. Results

4.1. Geomorphological analysis of the Paraguay-Corumbá Fluvial Plain

The PCFP consists of geomorphological compartments occupied by lakes, rivers, ephemeral and permanent small channels interconnecting floodplain to the river (“corixos” and “vazantes” in the local terminology according to Assine et al., 2015c), paleochannels, scroll bars drained by a system of anastomosed channels formed by the Paraguay, Paraguay-Mirim, and Corixo Fundo rivers. Its main compartments are a) floodbasin b) paleomeander belt, and c) meander belt (Figure 2).

The PCFP is bounded by adjacent fluvial plains and residual terrain. Its surface is marked by morphologies that show evidence of hydrological changes that have occurred in the area since the late Pleistocene (Macedo, 2013; Macedo et al., 2014).

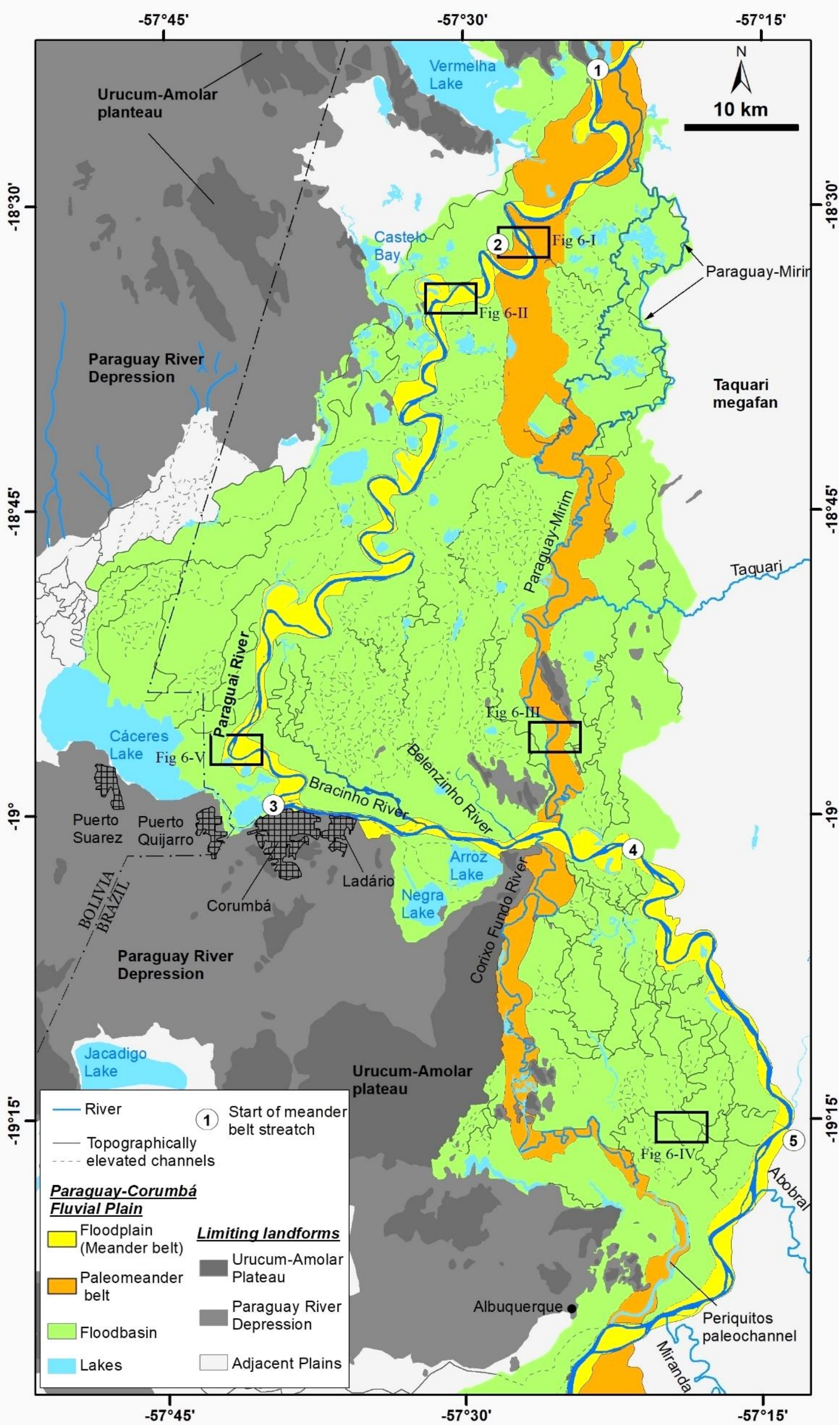

Figure 2. Geomorphological compartments of the PCFP. The geomorphological compartments mapped are meander belt (yellow), paleomeander belt (orange) and (floodbasin (green). The gray-toned areas represent the landforms that limit the PCFP. Coordinates in the WGS-84 datum.

The existence of paleolandforms composed of channels with levees (topographically elevated channel landforms, similarly to described by Trenhaile (2016)) in almost the entire PCFP is noteworthy. The meander belts represent the most important record of paleohydrological changes in this plain. The abandoned meander belt shows the change that occurred in the Paraguay River as the product of the river's avulsion at the latitude of Castelo Bay.

4.1.1. Floodbasin

The floodbasin is a flat surface negative relief that favors the accumulation of water common in large alluvial rivers floodplain (Lewin and Ashworth, 2014, Leli and Stevaux, 2020). In this case, flooding is conditioned by overflow of the Paraguay River during flood periods. In a longer rainy season, flooding can start with the rise of the water table, even before the river water overflows. The floodbasin is poorly drained, with water accumulation in swamps and lakes. However, a floodbasin may be drained by an internal drainage channel network (Lewin and Ashworth, 2014, Drago et al., 2008). In this case, the drainage network is formed by *corixos*, *vazantes*, and topographically elevated channels with 10 to 40 m width.

Corixos are intermittent (seasonal) river branches that can be dry for several years. They are watercourses of varied dimensions and flow intensity, and can be a swamp, channel, or even a watercourse that re-emerges during the flood season. They often occupy abandoned channels.

Vazantes are drainage lines from a flooded area into a marshy area to a river a small lake or ancient meander. *Vazantes* are broad, depressed, elongated extensions that connect contiguous waterbodies. During the flood season, they serve as outlets between waterbodies, acquiring an intermittent character. During the dry season, many stretches of *vazantes* can have a perennial character, presenting a humid soil, which would be linked, probably, to the proximity of the water table (Bazzo et al., 2012).

Topographically elevated channels are floodplain channels that develop natural levees, remaining higher (suspended) in relation to the general level of the floodbasin. They were defined for the first time by Assine (2015) in the Paraguay River floodbasins. These landforms have channels with levees, visible in the images and DEM (Figure 3). The flooding process tends to obliterate the existing forms in the floodbasin. However, it was possible to identify the drainage network formed by the topographically elevated channels (Figure 2). The meander belts truncated the drainage network.

In the southernmost portion of the PCFP, the channels in the floodbasin converge to form larger channels that in some cases develop scroll bars (Figure 4). However, a closer analysis of these landforms showed that these meandering channels have characteristics that differ from those presented by the paleomeander belt that is embedded in the floodbasin. The main differences of the features of the floodbasin to the paleomeander belt ones is that those of the floodbasin are more obliterated, and are not as embedded in the plain as those in the paleomeander belt.

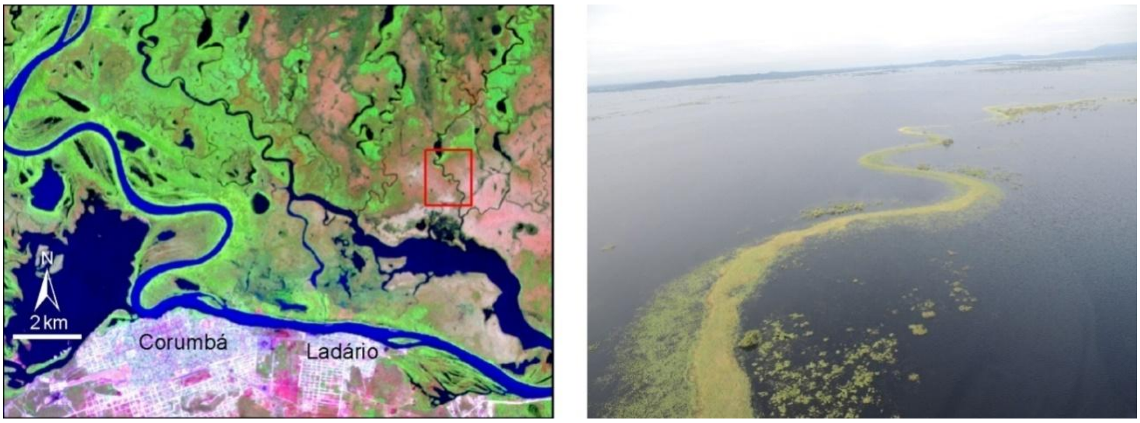

Figure 3. A topographically elevated channel at the Paraguay River floodbasin. Left: General view (rectangle is the detail photo) Source: Landsat 7 ETM+ image (R6G3B5); right: Oblique aerial view of a topographically elevated channel: very low and poorly-defined marginal levees formed by mud and vegetation separate the channel from the floodbasin.

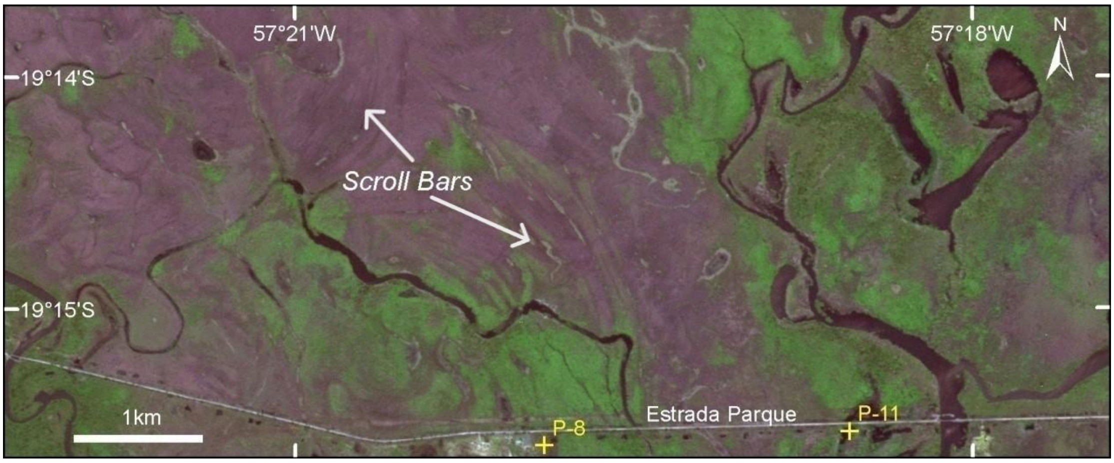

Figure 4. Sinuous channels with lateral migration marks (scroll bars) in the Paraguay River floodbasin. Source: RapidEye R1G2B3 image. Coordinates in the WGS-84 datum.

4.1.2. Paleomeander belt

Macedo et al. (2014) described the occurrence of paleomeander belts in the PCFP. In this study, we identified a well-defined paleomeander belt in the N-S direction. It was formed by scroll bars, paleochannels, and elongated ponds.

The average width of the paleochannel in the paleomeander belt is 170 m, which is 1.54 times smaller than those in the Paraguay River in the studied area (Macedo, 2017). Using Equation 1, we estimated an annual mean discharge of 1,354.11 $m^3 s^{-1}$ to the paleochannel belt (reach 1 in Figure 2 and Table 2), a value similar to that of the current Paraguay River.

The Paraguay-Mirim River flows within the paleomeander belt. This river rises on the left bank of the Paraguay River, at the latitude of the Vermelha Lake, with a width of approximately 75 m and a mean discharge of ~138 $m^3 s^{-1}$, and receives water from the Taquari Megafan and the Taquari River itself, in its course north-south (Figure 2). At its mouth on the Paraguay River, approximately 25 km downstream of the city of Corumbá, the Paraguay-Mirim River is 95 m wide with an average flow of ~238 $m^3 s^{-1}$.

The paleomeander belt is cut by the current meander belt of the Paraguay River at the mouth of the Paraguay-Mirim River. This geomorphological compartment is drained by the Corixo Fundo River on the right bank of the Paraguay River (Figure 2). The paleomeander belt ends in the Albuquerque district, in the Periquitos paleochannel, close to the confluence of the Miranda River, where it is again truncated by the current Paraguay River belt (Figure 2).

During flood periods, the paleomeander belt is flooded and part of the floodwater is retained in this geomorphological compartment, which returns the water to the Paraguay River at the mouth of the Paraguay-Mirim River (see supplementary material in: https://link.ufms.br/meanderflood).

4.1.3. Meander belt

A meander belt of the Paraguay River was identified. This meander belt consists of several geomorphological elements, including the Paraguay River channel, ponds, scroll bars, and islands. In the meander belt, we recognized several abandoned meanders by neck and chute cutoff, with the first type occurring more frequently.

The current meander belt of the Paraguay River was subdivided into five reaches according to the direction, width of the meander belt, sinuosity and slope of the channel (Table 2). The sinuosity of the Paraguay River decreases downstream, and the river plain is narrow and embedded at the Paraguay River floodbasin (Figure 2).

Table 2. Morphometric parameters for each section of the current meander belt of the Paraguay River. The slope was measured through the Digital Elevation Model (See Figure 2 for localization).

Reach	Sinuosity	Mean width (km)	Slope (cm/km^{-1})	Direction
1	1.62	1.18	3.99	SSW/NNE
2	1.78	1.82	2.94	SSW/NNE
3	1.29	1.29	2.88	ESE/WNW
4	1.38	1.49	2.44	SSE/NNW
5	1.19	1.61	2.56	SSW/NNE

The sharp deflection of the river to the east in its third reach has been attributed to structural control by a fault at the plain's border (Assine and Soares, 2004). This interpretation is consistent with regional lineament analyses that have identified a pervasive NNE/SSW structural system controlling drainage patterns across the Pantanal, likely related to reactivation of basement structures during the Quaternary (Paranhos Filho et al., 2013).

The third reach is conditioned by a fault at the margin of the plain (Figure 5). The current meander belt cuts the paleomeander belt in its first reach, in the northern part of the study area, in the third reach, at the confluence with the Paraguay-Mirim River, and in the fifth reach after confluence with the Miranda River (Figure 2).

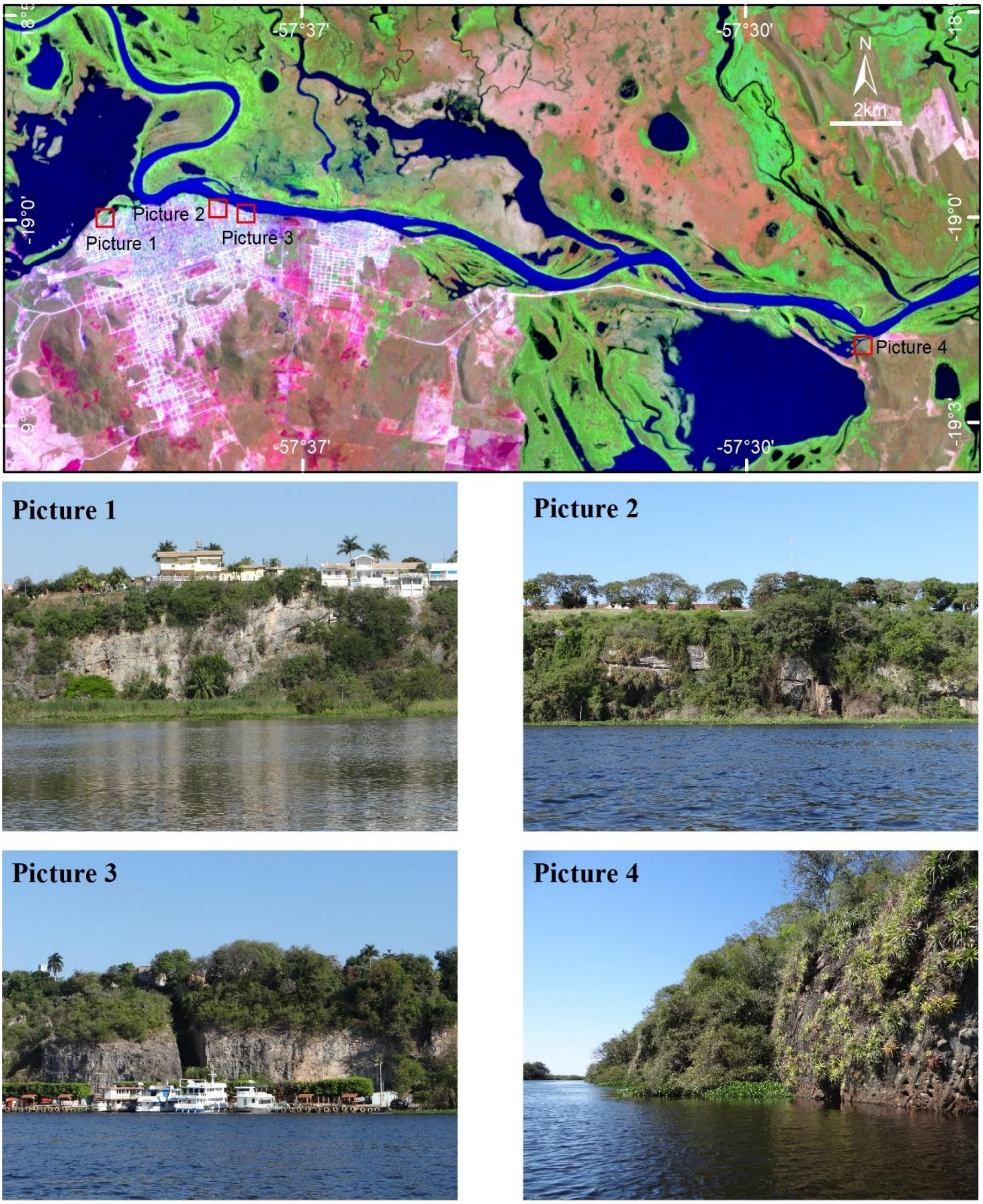

Figure 5. The Paraguay River channel is controlled by an E-W fault at the border of the plain in Corumbá, MS (Assine and Soares, 2004; Paranhos Filho et al., 2013). Photos 1 to 4: E-W fault escarpment exposing Precambrian rocks of the basement (08/05/2014). Image Landsat 7 ETM+ (R6G3B5). Coordinates in the WGS-84 datum.

4.2. *Geochronology and sedimentology*

The cores obtained in fieldwork are presented in Figure 6, Table 3 and in the supplementary material.

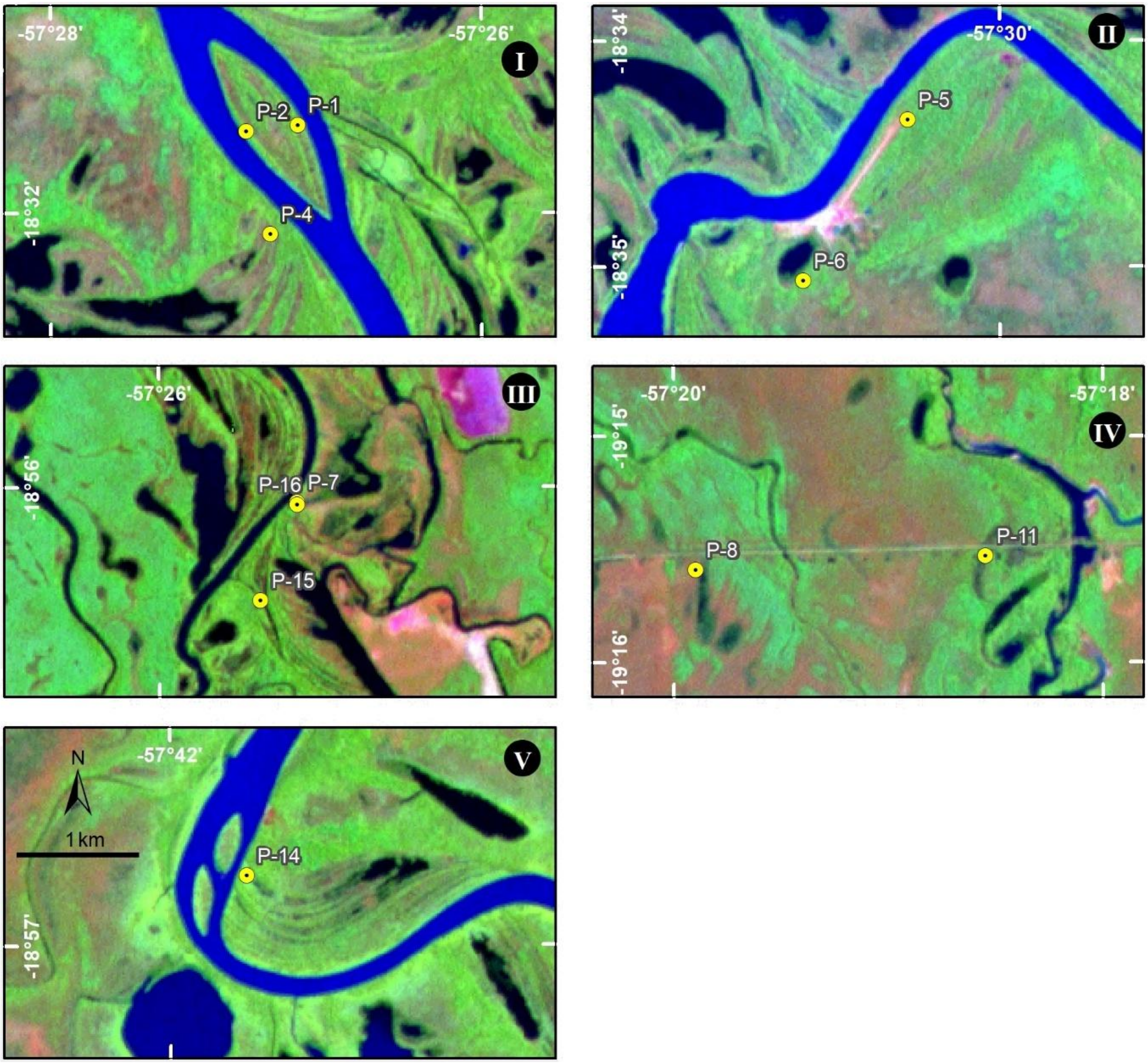

Figure 6. Detail of core sites (ETM+ image). P1, P2, P5 and P14 – meander belt; P6 – Floodbasin; P7, P15 and P16 – paleomeander belt; P8 and P11 – meandering channel in floodbasin. Coordinates in the WGS-84 datum.

4.2.1. Sedimentology

The cores P-8 and P-11 obtained in meandering channels in the floodplain (Figure 6 and Supplementary Material – P-8 and P-11) show a discrete upward-fining sequence, starting with very fine sand layers at the base (Sm facies) and transitioning to interlaminations of very fine sand and mud (S/F facies), deposited in a point bar environment.

In the paleomeander belt, the maximum depth obtained was 3.45 m and the minimum was 1.38 m. The paleomeander belt was surveyed at two different locations. The first location was near Laranjeira Island, 110 km upstream of the city of Corumbá (P1 and P2). The second was on the Paraguay-Mirim River 11 km upstream of its mouth with the Paraguay River (P7, P15 and P16). The paleomeander belt has a predominance of very fine sand to silty sand sediments (Sm and Fm facies). The presence of organic matter is another notable feature of this depositional association. Vegetal remains or organic layers were found in one of the cores recovered from that compartment (Fm(o) facies). The cores of the paleomeander belt (Figure 6 and Supplementary Material) presented facies with alternating silt and sand (S/F). The P-4 core presented, in its basal portion, alternation of thicker deposits with coarser deposits.

Profiles obtained in the meander belt show a predominance of facies of fine to very fine sand with massive structure and gray color (Sm facies). The presence of bioturbation by roots is constant, together with brown and red mottling (Supplementary Material F-2). The sediments of P-1 and P-2 are related to bar deposits that formed in the center channel (mid-channel bar) and that today has established itself as an island. The P-2 core consists of very fine white sand deposited in the channel (Sm facies:) in the base (1.34 - 1.48 m depth), covered by silty sand (1.26 – 1.34 m depth). Core sequence in ended by 0 – 0.17 m of light gray silt with vegetal fragments (Fm(o) Facies.

4.2.2. Chronology of the deposits

Data using the OSL/SAR method were obtained from 15 samples from the eleven coring sites (Table 3). The ages from the meander belt indicate that this morphological association has a late Holocene age (349–1,546 years). See the supplementary material for further details

Table 3. Core site localization, depth and OSL ages of samples (geographical coordinates referenced to the WGS-84 datum. *The abbreviations MB, PB, and FB stand for "meander belt," "paleomeander belt," and "floodbasin," respectively.

Sample	Comp*	Depth (m)	Number of aliquots	OD (%)	D_e (Gy)	Dose rate (Gy/ka^{-1})	Age (years)
P-1	MB	0.36	18/24	33	0.4±0	1.146±0.074	349±23
		1.31	19/24	39	0.9±0.1	1.008±0.061	893±113
P-2	MB	1.37	19/24	27	0.6±0	1.152±0.071	521±32
		1.44	12/24	20	0.3±0	0.503±0.029	596±35
P-4	PB	0.42	19/21	17	1.8±0.1	1.165±0.077	1,545±134
		1.00	20/24	17	2.1±0.1	1.072±0.066	1,958±153
		1.56	24/24	23	2.1±0.1	1.334±0.083	1,575±123
P-5	MB	1.33	24/24	30	1.9±0.1	1.344±0.104	1,414±132
P-7	PB	1.35	20/20	3	7.7±0.1	1.907±0.146	4,038±314
P-8	FB	0.14	24/24	26	4.2±0.2	1.469±0.116	2,860±233
		1.26	22/22	7	25.6±0.4	1.162±0.077	22,032±1.505
P-11	FB	1.33	14/14	3	17.5±0.2	1.024±0.060	17,092±1.020
P-14	MB	3.93	23/24	8	0.642±0.012	0.483±0.029	1,329±82
P-15	PB	2.93	19/24	13	0.246±0.008	0.300±0.016	819±51
P-16	PB	3.45	22/22	8	3.75±0.06	0.379±0.022	9,902±588

The samples taken in the meandering channels of the floodbasin (P-8 and P-11) revealed old ages, close to the Last Glacial Maximum (LGM), indicating that among our samples, the oldest one was found on floodbasin and that its deposits have late Pleistocene age (16,072 – 23,537 years).

The OSL ages obtained for the paleomeander belt indicate activity during the early Holocene (ca. 10.5–9.3 ka), with the belt remaining active until the late Holocene (core P-4, ~1.5 ka). The age obtained for core P-4 indicates that both belts were active during this period. Other possibility is the reworking of materials of the paleomeander belt by the recent fluvial dynamics. The samples collected in this core showed age overlap, most likely due to problems with the humidity values of the sample, as this parameter greatly affects the dose rate values.

5. Discussion

5.1. Chronostratigraphy and paleoenvironmental implications

The OSL chronology establishes a robust framework for the evolution of the PCFP. The finding that the floodbasin and its topographically elevated channels are the oldest features (>23 ka) indicates that this geomorphological compartment represents the foundational phase of the plain's evolution. The formation of these channels under a regime of high sediment supply is supported by their very nature – channels that aggrade their beds and build levees, becoming elevated above the floodbasin (Assine, 2015). This period coincides with the drier conditions inferred for the region prior to and during the Last Glacial Maximum, as suggested by pollen and diatom assemblages indicating a landscape dominated by grasses and herbs (Metcalfe et al., 2014; Whitney et al., 2011). Speleothem records further indicate that this drying was not uniform across the continent, with evidence for a significant drying in eastern Amazonia but more stable or modestly wetter conditions in the west during the LGM (Cheng et al., 2013). This scenario of reduced forest cover would have favored higher sediment yield, contributing to the aggradation of these channels. The convergence of these channels into meandering forms with scroll bars in the southern PCFP, dated to between 23.5 and 16 ka, indicates a dynamic system. This timing aligns with a period of increased precipitation suggested by speleothem records from central Brazil (Novello et al., 2017) and wider Amazonia (Cheng et al., 2013), which indicate a strengthening of the South American Summer Monsoon (SASM) around this time. As demonstrated by Cruz et al. (2009), increased austral summer insolation strengthens the SASM, leading to enhanced convective activity over tropical South America. This mechanism provides a robust climatic framework for the increased, yet still seasonal, discharge necessary to form the meandering reaches within the broader anabranching system of the PCFP floodbasin during the late Pleistocene.

5.2. Fluvial metamorphosis and avulsion dynamics

The activity of the paleomeander belt around 9.9 ka (OSL) marks a significant phase in the Paraguay River's behavior, although its initial formation may have occurred earlier during the late Pleistocene, as illustrated in the evolutionary model of the PCFP (Figure 7). The paleodischarge estimate of approximately 1,354 $m^3\ s^{-1}$ for the paleomeander belt, derived from channel morphometry, suggests that the former Paraguay River operated under a flow regime very similar to its modern counterpart. This similarity in discharge, yet marked difference in channel pattern (a wider, aggradational belt versus the current entrenched one), is a key finding. It implies that the fundamental change in fluvial style was not driven by a simple increase in water volume. Instead, the shift must have been primarily controlled by other variables, most notably a change in sediment flux and its calibre, or a change in the spatiotemporal distribution of discharge (e.g., peak versus mean flow). A reduction in sediment load relative to discharge would favor the lateral mobility and suspended-load deposition characteristic of meandering rivers, potentially explaining the formation of the extensive paleomeander belt. This interpretation aligns with regional records from the Pantanal indicating the expansion of tropical forest and stabilization of floodplain environments during the late Pleistocene to early Holocene transition (Whitney et al., 2011), which would have contributed to increased catchment stability and, theoretically, reduced sediment supply.

This shift towards a persistent meandering pattern may reflect a reorganization of fluvial dynamics under the hydrological conditions of the early Holocene. However, regional paleoclimate records indicate that the early to mid-Holocene (ca. 9–6 ka) was relatively dry in the Pantanal (Fornace et al., 2016), and speleothem records from central-western Brazil also show drier conditions compared to the late Pleistocene (Novello et al., 2017). In contrast, speleothem records from subtropical Brazil suggest a weaker South American Summer Monsoon and more variable hydroclimate during the early to mid-Holocene (Cruz et al., 2009). These apparently drier conditions may have been accompanied by channel avulsions and local geomorphic adjustments that led to the formation of the paleomeander belt, rather than an overall increase in discharge. Alternatively, the paleomeander belt could have been initiated under wetter conditions in the late Pleistocene and remained active until ca. 9 ka. The subsequent establishment of more humid conditions after ca. 6 ka (Fornace et al., 2016) in the late Holocene would then have provided the stable discharge required for the construction of the new meander belt. The establishment of lake conditions in Castelo Bay around 6.5 ka (Bezerra and Mozeto, 2008) also points to a transition to more stable hydrological conditions in the mid-Holocene, creating an environment conducive to the aggradation of the wide meander belt.

The subsequent avulsion that led to the current meander belt (~2–1.5 ka), represented in Figure 7C, can be interpreted as a natural consequence of the long-term aggradation within the paleomeander belt. As the belt built upwards, the river would have become increasingly prone to avulsion, a process widely recognized in the Pantanal and other South American fluvial systems like the Bolivian Chaco and the Salado/Juramento megafan (Assine, 2005; Latrubesse et al., 2012; Thalmeier et al., 2021). The fact that the current belt is entrenched suggests the avulsion occurred at a topographically favorable location, giving the new channel sufficient energy to incise itself into the pre-existing floodplain. This avulsion event may be linked to a return to a more seasonal climate after the dry late Holocene (ca. 3.5–1.4 ka BP), as described by Iriondo and Kröhling (2022) for other fluvial systems in the region, which can increase sediment delivery and accelerate channel-filling processes, ultimately triggering avulsion.

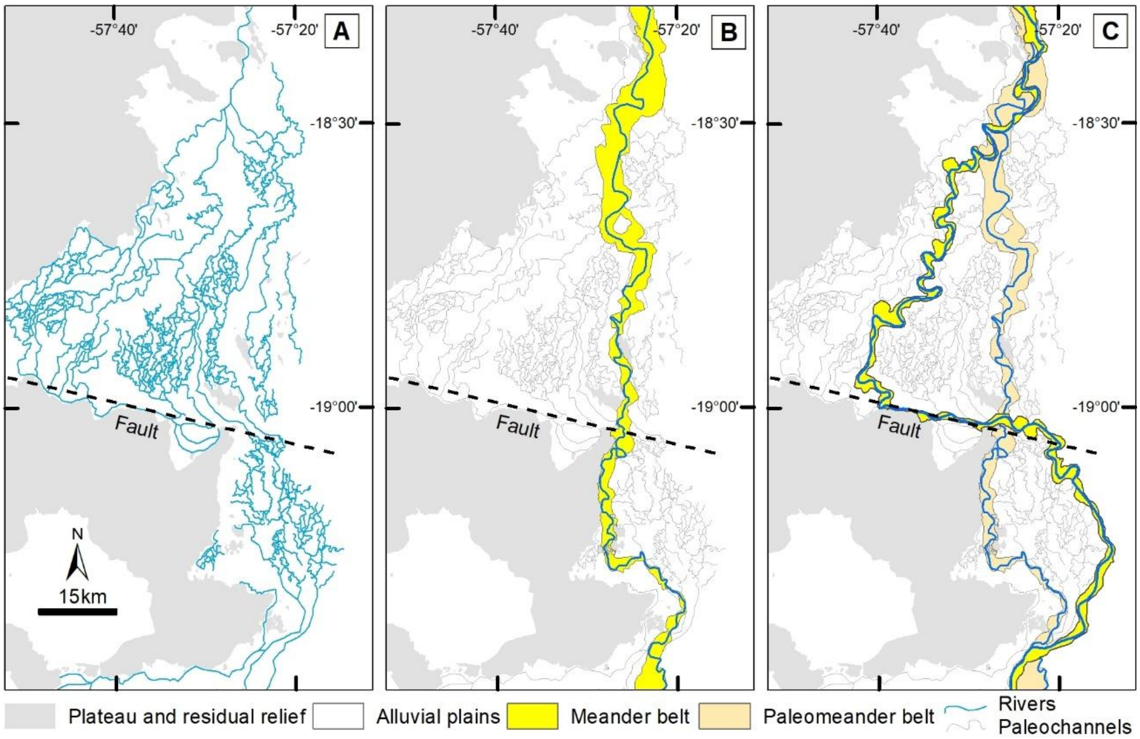

Figure 7. Evolutionary scheme of the PCFP. A) a topographically elevated channel drainage network spread on the floodplain (approximately 23.5 ka until 10 ka); B) a N-S meander belt was active between ca. 10 and 2 ka (OSL ages), truncating the former topographically elevated channel pattern; its initial formation likely occurred during the late Pleistocene (ca. 19–12 ka) under wetter conditions; C) an avulsion event changed the river course to the SSW where the Paraguay-Mirim river is installed, with progressive abandonment of the former meander belt (2 ka). The Paraguay River is controlled by a tectonic lineament (fault) at the basin border near the city of Corumbá and cuts its former meander belt near the Negra and Arroz Lakes, truncating it again just after the mouth of the Miranda River. Coordinates in the WGS-84 datum.

5.3 Regional correlation and climatic controls

The evolutionary model proposed for the PCFP is consistent with and helps to refine the regional paleohydrological framework for the Pantanal. The ages obtained for the meandering channels within the floodbasin (22–17 ka) are contemporary with the braided channel deposits identified in the Cuiabá and São Lourenço megafans (Pupim, 2014; Pupim et al., 2017). This contemporaneity strengthens the interpretation of a regional climatic driver for fluvial activity during the late Pleistocene (ca. 49–19 ka), while the different channel patterns (meandering in the trunk river vs. braided in the megafans) highlight how the same climate can produce different geomorphic responses depending on the position in the sedimentary system, a phenomenon also observed in the Chaco plains (Latrubesse et al., 2012; Thalmeier et al., 2021). This spatial heterogeneity in fluvial response is consistent with the complex patterns of precipitation variability documented for tropical South America on orbital timescales. Speleothem records have revealed a dipole-like antiphasing of precipitation, where increased monsoon intensity over western Amazonia and southern Brazil is accompanied by large-scale subsidence and aridity over northeastern Brazil (Cruz et al., 2009). Similarly, a dipole pattern between western and eastern Amazonia has been documented for the last glacial period (ca. 115–11.7 ka; Cheng et al., 2013). Quantitative estimates from speleothems in eastern Amazonia indicate that precipitation during the Last Glacial Maximum (LGM, ~21 ka) was only ~58% of modern levels, while during the mid-Holocene (ca. 6 ka) it reached ~142%, demonstrating the magnitude of these orbital-scale hydroclimate changes (Wang et al., 2017). Such regional variability in hydroclimate may have differentially affected sediment and water supply to various parts of the Pantanal basin, contributing to the divergent fluvial responses observed between the trunk river and its tributary megafans.

Crucially, paleoclimate records from western Amazonia itself indicate that this region did not experience extreme or prolonged aridity during the last glacial period. Mosblech et al. (2012), based on a speleothem $\delta^{18}O$

record from Ecuadorian Amazonia spanning the past 94 kyr, concluded that ecosystems in western Amazonia have not experienced prolonged drying, despite millennial-scale variability linked to North Atlantic forcing. This contrast between western and eastern Amazonia (Wang et al., 2017; Cheng et al., 2013) highlights the complex spatial heterogeneity of South American hydroclimate and is particularly important for the interpretation of the PCFP record, as it suggests that the headwater regions of the Paraguay River system in the Andes and western Amazonia likely remained a significant source of moisture and runoff throughout the late Pleistocene (ca. 94–11.7 ka) , even as eastern areas experienced pronounced drying — a scenario consistent with the sustained, though variable, fluvial activity recorded in the floodbasin sediments.

A high-resolution paleolimnological record from Lake Negra, a floodplain lake located in the same geomorphic compartment of the Paraguay River, provides further independent support for this evolutionary sequence. Rasbold et al. (2019) documented environmental changes that closely mirror the phases identified in the PCFP. Their record shows that the late Pleistocene – between approximately 19 and 12 cal ka BP – was characterized by strong fluvial influence under an intense monsoon, with deposition of massive sands, consistent with the high-energy conditions inferred for the formation of the PCFP floodbasin. The period from approximately 11 to 5,7 cal ka BP (early to middle Holocene) saw the establishment of a stable, perennial lake with high organic carbon content and well-preserved sponge spicule assemblages, indicating environmental stability and isolation from the main river channel, which aligns with the development of the paleomeander belt in the PCFP. A pronounced hiatus from ~5.7 to 3.0 cal ka BP in the Lake Negra record provides compelling evidence for a severe mid-to-late Holocene drought that desiccated the lake floor, corroborating regional speleothem data and supporting the interpretation of increased aridity that may have contributed to channel aggradation and avulsion in the Paraguay River system. The re-establishment of lacustrine conditions after ~1.0 cal ka BP in Lake Negra coincides with the formation of the active meander belt in the PCFP, suggesting a return to wetter conditions similar to the present.

Further west, a multi-indicator study of a sediment core from Lake Cáceres (Bolivia), another large floodplain lake connected to the Paraguay River, provides additional insights into middle Holocene environmental conditions. Rasbold et al. (2020) documented exceptionally high organic carbon burial (~15 wt%) between 7.3 and 6.0 cal ka BP, which they attributed to relatively dry conditions and diminished seasonal flooding that led to hydrologic closure of the lake. Under these conditions, floating macrophyte mats colonized the expanded shallow margins, and organic matter accumulation occurred in situ without being exported to the Paraguay River. This interpretation is particularly relevant for the PCFP evolution, as it demonstrates that the middle Holocene was characterized by reduced fluvial connectivity and lower energy conditions, consistent with a phase of aggradation within the paleomeander belt that may have preconditioned the system for the subsequent avulsion event that formed the current meander belt.

The regional significance of this evolutionary pattern is reinforced by studies from the upper Paraná River, the trunk river that receives all drainage from the Paraguay River system. Stevaux (1994), based on geomorphological, sedimentological, and palynological analyses of the Upper Paraná River fluvial plain, proposed a Quaternary evolution model that closely parallels the sequence documented in the PCFP. He identified a late Pleistocene phase (>40 ^{14}C ka BP) of valley filling by braided river deposits and colluvium, corresponding to the formation of the PCFP floodbasin (>23 ka). This was followed by a major transition to a meandering system between 6,000 and 4,000 ^{14}C yrs BP (Stevaux, 1994), which calibrates to approximately 7.2–4.2 cal ka BP (calibrated with OxCal v4.4 [Bronk Ramsey, 2009] using the IntCal20 curve [Reimer et al., 2020]; see Supplementary Material SM 4 for detailed calibration results). In contrast, the paleomeander belt of the PCFP formed earlier, between 10 and 9 ka (OSL, calendar years). This temporal lag (see explicit comparison below) reflects the antiphase hydroclimatic forcing between western and eastern Amazonia (Cheng et al., 2013; Cruz et al., 2009), where the western headwaters of the Paraguay River became wetter earlier than the eastern headwaters of the Paraná.

Thus, the parallel evolutionary trend (from aggradational to meandering systems) is evident in both rivers, but the timing is not parallel: the Paraguay shifted ~3–4 kyr earlier than the Paraná. This difference does not diminish the importance of regional climate as a primary driver; rather, it highlights how the same climate forcing can produce diachronous fluvial responses due to the spatial heterogeneity of precipitation regimes across tropical South America.

In another work about the Paraná River, Stevaux (2000) synthesized paleoclimatological data from the Upper Paraná River and proposed a sequence of four climatic episodes that provides a robust regional framework for understanding the PCFP evolution. He defined a First Drier Episode (>40,000–8,000 ^{14}C yrs BP – original data from the article, not calibrated) characterized by aeolian activity and braided river systems under semi-arid conditions, consistent with the formation of the PCFP floodbasin (>23 ka OSL). This was followed by a First Wetter Episode (8,000–3,500 ^{14}C yrs BP), which calibrates to approximately 9.1–3.6 cal ka BP (using OxCal v4.4. (Bronk Ramsey, 2009) and the IntCal20 curve (Reimer et al., 2020). This episode, marked by forest expansion and a shift to anastomosed river patterns, corresponds to the development and activity of the paleomeander belt of the PCFP (ca. 10–9 ka OSL). A Second Drier Episode (3,500–1,500 ^{14}C yrs BP), calibrating to approximately 3.6–1.3 cal ka BP, is indicated by decreased organic content and alluvial fan activity, aligning with a phase of channel aggradation that may have preconditioned the Paraguay River for avulsion. Finally, the Second (Present) Wetter Episode (1,500 ^{14}C yrs BP to present), which calibrates to ca. 1.5–1.3 cal ka BP to present, records the return to humid conditions similar to the modern climate, coinciding with the formation of the active meander belt in the PCFP (ca. 1.5–0.35 ka OSL). This remarkable parallelism between the climatic history of the Paraná and Paraguay river basins underscores the primary role of regional climatic changes in driving fluvial evolution during the Late Quaternary.

This evolutionary history is remarkably consistent with paleoenvironmental reconstructions from neighboring regions across the southern and western margins of the Pantanal. In the Argentine plains, Iriondo and Garcia (1993) documented an arid and cold phase between 18,000 and 8,500 ^{14}C yrs BP (uncalibrated), which corresponds approximately to a calendar interval of 21,500 to 9,500 cal yrs BP (approximate calibration using IntCal20; Reimer et al., 2020), characterized by aeolian deposition, which aligns with the conditions inferred for the formation of the PCFP floodbasin and its suspended channels prior to and during the LGM. They subsequently documented a humid subtropical phase between 8,500 and 3,500 ^{14}C yrs BP (uncalibrated), which corresponds, after calibration, to an interval of approximately 9,500 to 3,800 cal yrs BP (calibration using IntCal20; Reimer et al., 2020), marked by pedogenesis and enhanced fluvial dynamics in the Argentine plains.

The OSL ages obtained for the paleomeander belt indicate activity during the early Holocene (ca. 10–9 ka). However, multiple paleoclimate records from the Pantanal and central Brazil document that this period was characterized by drier conditions compared to the late Pleistocene (Whitney et al., 2011; McGlue et al., 2012; Novello et al., 2017). This apparent contradiction raises the possibility that the OSL ages do not capture the onset of meander belt formation, but rather represent the middle to final stages of activity or sediment reworking within an older landform. The estimated paleodischarge for the paleomeander belt, derived from channel morphometry, suggests a flow regime similar to the modern Paraguay River, which is difficult to reconcile with a dry early Holocene climate. Therefore, we hypothesize that the initiation of the paleomeander belt likely occurred earlier, during the late Pleistocene (possibly between 19 and 12 ka), when regional records indicate wetter conditions (Whitney et al., 2011) and higher monsoon intensity (Cheng et al., 2013; Novello et al., 2017). The available OSL ages, obtained from a single core at 3.5 m depth, may not represent the basal deposits of this geomorphological unit, leaving the timing of its inception unresolved. Future dating of deeper cores or of basal channel deposits is needed to test this hypothesis.

Similarly, in the Bolivian Chaco, May et al. (2008) reported coarse fluvial deposits from braided systems prior to and during the LGM (≥22.2–18 cal ka BP), indicating high-energy conditions with low vegetation cover, followed by the development of well-developed paleosols during the Lateglacial (ca. 18–11.5 cal ka BP), signaling a shift to geomorphic stability and wetter conditions. This sequence closely mirrors the transition to the paleomeander belt system in the PCFP at the end of the Pleistocene. The subsequent return to fluvial and fluvio-aeolian sedimentation in the Bolivian piedmont during the Mid-Holocene (ca. 10–2.9 cal ka BP), followed by renewed stability and soil formation after ~2.9 cal ka BP, provides a coherent regional backdrop for the avulsion event that led to the current meander belt in the PCFP and its late Holocene activity.

While these regional records consistently point to a mid-to-late Holocene shift towards wetter conditions and landscape stability, the timing of specific geomorphic responses, such as fluvial avulsions, appears to vary within the Pantanal itself. The younger age of the current meander belt in the PCFP (~1.5 ka) compared to the meander belt in the Nabileque area (~6.5 ka; Kuerten, 2010) suggests that while climate may provide the overarching control, the timing of avulsive events is also influenced by local autogenic factors and complex system responses, as discussed in models of fluvial evolution for the region (Iriondo and Kröhling, 2022). Therefore, the PCFP record demonstrates that the Pantanal's fluvial history is a product of regional climatic changes acting upon a complex landscape where local sedimentology and topography dictate the specific timing and expression of system-wide changes.

However, it is important to consider that this chronological comparison involves datasets produced with different luminescence dating protocols. Kuerten (2010) likely employed a Multiple Aliquot Additive Dose (MAAD) protocol, which was standard prior to the development of the SAR protocol used in this study (Murray and Wintle, 2000). The SAR protocol offers significant advantages, including correction for sensitivity changes and more rigorous quality control (e.g., dose recovery tests, recycling ratios). As a result, the MAAD ages, particularly for older samples, may carry larger systematic uncertainties and are potentially less accurate than the SAR ages presented here (Wintle and Murray, 2006). Therefore, while the relative sequence of events (Nabileque avulsion preceding the PCFP avulsion) is stratigraphically coherent and likely correct, the precise age of ~6.5 ka for the Nabileque meander belt should be viewed with appropriate caution.

6. Conclusions

The PCFP is a Quaternary continental sedimentation area that provides significant evidence of environmental changes, with the paleomeander belt serving as an important record of climate shifts in the Paraguay River floodbasin. The landforms help us understand the evolution of the Pantanal.

This plain consists of geomorphological compartments bordered by adjacent plains and the basin's bedrock, influencing the river's behavior. The recognized landform associations indicate paleoclimatic changes that affected the fluvial system, altering the Paraguay River's style in response to hydrosedimentary conditions and global climate changes, likely associated with glacial stages.

Results show that the PCFP comprises: 1) a paleomeander belt active from the late Pleistocene through the early to late Holocene (ca. 10–9 ka to ~1.5 ka OSL), with its initial formation possibly predating the early Holocene; 2) an active meander belt formed in the late Holocene (ca. 1.5–2 ka); and 3) a floodbasin with topographically elevated channel paleoforms formed before the LGM (>23.5 ka). The current meander belt is 1.5 to 2 ka old, while the paleomeander belt remained active until just before the avulsion that led to the present channel.

The oldest morphologies in the PCFP, represented by the floodbasin with its topographically elevated channels (late Pleistocene, >23 ka), record a period of high sediment supply and variable discharge under predominantly drier climatic conditions prior to and during the LGM. At the end of the Pleistocene (from ca. 19 ka onward), rising temperatures and increased precipitation likely contributed to the initiation of a meander belt near the Taquari fan, which remained active through the early and middle Holocene until about 1.5 ka, despite drier conditions during the early Holocene.

Around 2 ka ago (^{14}C yrs BP), towards the end of a drier phase documented regionally (Stevaux, 2000), an avulsion process redirected the Paraguay River to its current course, initiating the formation of the active meander belt. The establishment of this new meander belt coincided with the return to wetter climatic conditions in the late Holocene, similar to the present, which allowed the river to develop its characteristic meandering pattern within an entrenched valley.

Thus, the evolution of the PCFP reflects changes in the river's fluvial pattern, avulsion, and abandonment of meander belts, influenced by regional climate change. The analysis of depositional forms and dating provided clearer insights into the area's morphologies over geological time.

Author’s contributions: Conception, Hudson Macedo and José Stevaux.; methodology, Hudson Macedo.; software (GIS), Hudson Macedo; validation, Hudson Macedo, José Stevaux and Mario Assine; formal analysis, Hudson Macedo, José Stevaux and Mario Assine; research, Hudson Macedo, Aguinaldo Silva; resources, Aguinaldo Silva, José Stevaux and Mario Assine.; data preparation, Hudson Macedo; article writing, Hudson Macedo and José Stevaux; revision, Hudson Macedo, José Stevaux and Mario Assine; supervision, José Stevaux; acquisition of funding, Aguinaldo Silva, José Stevaux and Mario Assine. All authors have read and agreed with the published version of the manuscript.

Data Availability: The supplementary material accompanying this work is available at: Macedo, H. (2026). Supplementary material. In Revista Brasileira de Geomorfologia. Zenodo. https://doi.org/10.5281/zenodo.20528169. The map in Geopackage format can also be accessed at the following address: https://doi.org/10.5281/zenodo.20528814.

Funding: This research was funded by National Council for Scientific and Technological Development (CNPq), grant number 443437/2014-9; São Paulo Research Foundation (FAPESP), grant number 14/06889-2; National Council for Scientific and Technological Development (CNPq), grant number 405131/2025-9, 406582/2023-8; Fundação de Apoio ao Desenvolvimento do Ensino, Ciência e Tecnologia do Estado de Mato Grosso do Sul (FUNDECT), grant numbers 063/2017, 267/2022, 172/2023, 342/2024, 111/2024.

Acknowledgments: We are grateful to the Gamma Spectrometry and Luminescence Laboratory (LEGaL), Department of Sedimentary and Environmental Geology, University of São Paulo (USP), under the coordination of Professor André Sawakuchi, which made possible not only the dating of the deposits mapped in this work but also the technical training and scientific development. We thank the Federal University of Mato Grosso do Sul (UFMS), Pantanal campus, Ecologia em Ação (ECOA), and the Acácia Institute for their support during the fieldwork campaigns. We thank the Coordination for the Improvement of Higher Education Personnel (CAPES) for granting the doctoral scholarship, which supported the first author from August 2013 to February 2015. We thank the National Council for Scientific and Technological Development (CNPq) for granting the doctoral scholarship (Process No. 140334/2015-7), from March 2015 to August 2017. We also thank for the financial support provided to the research project "Hydro-sedimentological dynamics in an inherited multichannel system of the Paraguay River: a new paradigm for fluvial geomorphology" (Process No. 443437/2014-9).

Conflict of Interest: The authors declare not having any conflict of interest. The funders had no interference in the development of the study; in the collection, analysis, or data interpretation; in the writing of the manuscript, or in the decision to publish the results.

Declaration of Artificial Intelligence Use: During the preparation of this manuscript, the authors used the generative AI tool DeepSeek (DeepSeek-V3). This tool was employed exclusively for the following purposes: Grammatical revision and language fluency: to improve the clarity, coherence, and overall readability of the text, ensuring the English language usage was of appropriate scientific standard; Translation support: to assist with the translation of selected short excerpts from Portuguese to English during the manuscript's preparation; Data analysis and interpretation: to help interpret the Optically Stimulated Luminescence (OSL) data and to assist in the calibration of radiocarbon (^{14}C) ages cited from the literature, using the OxCal software and the IntCal20 calibration curve; Development and refinement of hypotheses: to help in the formulation and iterative refinement of interpretations and the geomorphological evolutionary model, based on the data and discussions from the other authors. All authors critically reviewed the content generated by the AI tool and made substantial intellectual contributions to the final version. After using this tool, all authors reviewed and edited the content as necessary and take full and joint responsibility for the final content of the publication. The authors also confirm that no AI-generated content was used without critical review, and that no generative AI tool is listed as an author or co-author of this work, in accordance with the journal's editorial policy and the Brazilian National Council for Scientific and Technological Development (CNPq) Ordinance No. 2.664/2026.

8. References

1. ALHO, C.J.R.; LACHER, T.E.; GONÇALVES, H.C. Environmental degradation in the Pantanal ecosystem. **Bioscience**, v.38, p.164–171, 1988.
2. ALMEIDA, F.F.M.. **Geologia do sudoeste Matogrossense**. Boletim do DNPM/DGM, v.116, p.1-118, 1945.
3. ANA/GEF/PNUMA/OEA. Diagnóstico analítico do Pantanal e Bacia do Alto Paraguai. In: **Implementação de práticas de gerenciamento integrado de bacia hidrográfica para o Pantanal e Bacia do Alto Paraguai**. Subprojeto 9.4A. Brasília, 2003.
4. ASSINE, M. L. **Sedimentação na bacia do Pantanal Mato-Grossense, Centro-Oeste do Brasil**. 105 f. Tese de Livre-Docência - UNESP, Rio Claro-SP, 2003.
5. ASSINE, M. L. River avulsions on the Taquari megafan, Pantanal wetland, Brazil. **Geomorphology**, v.70, p.357-371, 2005.
6. ASSINE, M.L. Brazilian Pantanal: A Large Pristine Tropical Wetland. In: Vieira B.C., Salgado A.A.R., Santos L.J.C. (ed.) **Landscapes and Landforms of Brazil** Springer Netherlands, (World Geomorphological Landscapes), 135-146, 2015.
7. ASSINE, M. L.; SOARES, P. C. Quaternary of the Pantanal, west-central Brazil. **Quaternary International**, v.114, p.23-24, 2004.
8. ASSINE, M. L.; SILVA, A. Contrasting fluvial styles of the Paraguay River in the northwestern border of the Pantanal wetland, Brazil. **Geomorphology**, v.113, p.189-199, 2009.
9. ASSINE, M. L.; PADOVANI, C.R.; ZACHARIAS, A.A.; ANGULO, R.J.; SOUZA, M.C. Compartimentação geomorfológica, processo de avulsão fluvial e mudanças do curso do rio Taquari, Pantanal Mato-Grossense. **Revista Brasileira de Geomorfologia**, v.6, n.1, p.97-108, 2005.
10. ASSINE, M.L.; CORRADINI, F.A.; PUPIM, F.N.; MCGLUE, M.M. Channel arrangements and depositional styles in the São Lourenço fluvial megafan, Brazilian Pantanal wetland. **Sedimentary Geology**, v.301, p.172-184, 2014. DOI: 10.1016/j.sedgeo.2013.11.007.
11. ASSINE, M.L.; MERINO, E.R.; PUPIM, F.N.; MACEDO, H.A.; SANTOS, M.G.M. The Quaternary alluvial systems tract of the Pantanal Basin, Brazil. **Brazilian Journal of Geology**, v.45, n.3, p.475-489. 2015a. DOI: 10.1590/2317-4889201520150014.
12. ASSINE, M.L.; MACEDO, H.A.; STEVAUX, J.C.; BERGIER, I.; PADOVANI, C.R.; SILVA, A. Avulsive Rivers in the Hydrology of the Pantanal Wetland. In: Ivan Bergier e Mario Assine (ed.), **Dynamics of the Pantanal wetland in South America**, Hdb Env Chem, v.37, p.83-110, 2015b. DOI: 10.1007/698_2015_351.

13. ASSINE, M.L.; MERINO, E.R.; PUPIM, F.N.;WARREN, L.V.; GUERREIRO, R.L.; MCGLUE, M.M. Geology and Geomorphology of the Pantanal Basin. In: Ivan Bergier e Mario Assine (ed.), **Dynamics of the Pantanal wetland in South America**, Hdb Env Chem, v.37, p.23-50, 2015c. DOI: 10.1007/698_2015_349
14. BALEK, J. **Hydrology and water resources in tropical regions**. Amsterdam: Elsevier, 1983.
15. BAZZO, J.C.; FREITAS, D.A.F.; SILVA, M.L.N.; CARDOSO, E.L.; SANTOS, S.A. Aspectos geofísicos e ambientais do Pantanal da Nhecolândia. **Revista de Geografia** (UFPE), v. 29, n. 1, p. 141-161, 2012.
16. BERGIER, I. Effects of highland land-use overlowlands of the Brazilian Pantanal. **Science of TheTotal Environment**, v.463-464, p. 1060-1066, 2013. DOI: 10.1016/j.scitotenv.2013.06.036.
17. BERGIER, I.; RESENDE, E. K. Dinâmica de cheias no Pantanal do rio Paraguai de 1900 a 2009. In: SIMPÓSIO DE GEOTECNOLOGIAS NO PANTANAL, 3., 2010, Cáceres. **Anais...** Campinas: Embrapa Informática Agropecuária; São José dos Campos: INPE, 2010. p. 35-43. Disponível em: https://www.geopantanal.cnptia.embrapa.br/2010/cd/p147.pdf. Acesso em: 15 fev. 2026.
18. BEZERRA, M. A. O.; MOZETO, A. A. Deposição de carbono orgânico na planície de inundação do rio Paraguai durante o Holoceno Médio. **Oecologia Brasiliensis**, v.12, n.1, p.155-171, 2008.
19. BRONK RAMSEY, C. Bayesian analysis of radiocarbon dates. **Radiocarbon**, v. 51, n. 1, p. 337-360, 2009. DOI: 10.1017/S0033822200033865.
20. CHASE, C.G.; SUSSMAN, A.J.; COBLENTZ, D.D. Curved Andes: geoid, forebulge, and flexure. **Lithosphere**, v.1, n.6, p.358-363, 2009.
21. CLARKE, R. T.; TUCCI, C. E. M.; COLLISCHONN, W. Variabilidade temporal no regime hidrológico da bacia do rio Paraguai. **Revista Brasileira de Recursos Hídricos**, Porto Alegre, v. 8, n. 1, p. 201-211, jan./mar. 2003. Disponível em: https://revistas.abrhidro.org.br/article.php?Article=559. Acesso em: 15 fev. 2026.
22. CHENG, H.; SINHA, A.; CRUZ, F.W.; WANG, X.; EDWARDS, R.L.; D'HORTA, F.M.; RIBAS, C.C.; VUILLE, M.; STOTT, L.D.; AULER, A.S. Climate change patterns in Amazonia and biodiversity. **Nat. Commun**., v.4, n.1411, p.1-6, 2013. DOI: 10.1038/ncomms2415.
23. CORRADINI, F.A. **Geomorfologia fluvial, mudanças ambientais e evolução do megaleque do rio São Lourenço, Quaternário do Pantanal Mato-Grossense**. Tese de Doutorado (Geociências e Meio Ambiente) - UNESP, Rio Claro-SP, 2011, 164p.
24. CRUZ, F.W.; VUILLE, M.; BURNS, S.J.; WANG, X.; CHENG, H.; WERNER, M.; LAWRENCE EDWARDS, R.; KARMANN, I.; AULER, A.S.; NGUYEN, H. Orbitally driven east-west antiphasing of South American precipitation. **Nat. Geosci**., v.2, p.210-214, 2009. DOI: 10.1038/ngeo444.
25. DEL'ARCO, J. O.; SILVA, R.H.; TARAPANOFF, I.; FREIRE, F.A.; PEREIRA, L.G.M.; SOUZA, S.L.; LUZ, D.S.; PALMEIRA, R.C.B.; TASSIRANI, C.C.G. Geologia - Folha SE.21 Corumbá e parte da folha SE.20. In: **Projeto RADAMBRASIL** - Levantamento de Recursos Naturais. Rio de Janeiro-RJ: MME/SG, 1982, v.27, p.25-160.
26. DRAGO, E. C.; WANTZEN, K. M.; PAIRA, A. R. The floodplain of the lower reach of the Paraguay River: geomorphologic and hydrological characteristics. **Ecohydrology & Hydrobiology**, v. 8, n. 1, p. 107-118, 2008. DOI: 10.2478/v10104-009-0004-1.
27. DULLER, G. A. T. Distinguishing quartz and feldspar in single grain luminescence measurements. **Radiation Measurements**, v. 37, n. 2, p. 161-165, 2003. DOI: 10.1016/S1350-4487(02)00170-1.
28. DURY, G. H. Theoretical implications of underfit streams. **United States Geological Survey Professional Paper**, 452-C, 1965, 43p. Disponível em: https://play.google.com/store/books/details?id=bx8fcauReI4C&rdid=book-bx8fcauReI4C&rdot=1&pli=1. Acesso em: 28 set 2025.
29. ETHRIDGE, F. G.; SCHUMM, S. A. Reconstructing paleochannel morphologic and flow characteristics: methodology, limitations, and assessment. In: **Fluvial Sedimentology VI**, Special Publication of the International Association of Sedimentologists, 2007, p. 703-721.
30. FACINCANI, E. M.; ASSINE, M. L.; SILVA, A.; ZANI, H.; ARAUJO, B. C.; MIRANDA, G. M. Geomorfologia fluvial do leque do rio Aquidauana, borda sudeste do Pantanal, MS. In: Simpósio de Geotecnologias no Pantanal, 1., 2006, Campo Grande-MS. **Anais...** Campo Grande: INPE, 2006. p.175-181.
31. FORNACE, K.L.; WHITNEY, B.S.; GALY, V.; HUGHEN, K.A.; MAYLE, F.E. Late Quaternary environmental change in the interior South American tropics: new insight from leaf wax stable isotopes. **Earth and Planetary Science Letters**, v.438, p.75-85, 2016. DOI: 10.1016/j.epsl.2016.01.007.
32. FRANCO, M. S.; PINHEIRO, R. Geomorfologia - Folha SE.21 Corumbá e parte da folha SE.20. In: **Projeto RADAMBRASIL**. Levantamento de Recursos Naturais. Rio de Janeiro: MME/SG, 1982, v.27, p.161-224. https://biblioteca.ibge.gov.br/visualizacao/livros/liv13270.pdf

33. FRYIRS, K. A.; BRIERLEY, G. J. **Geomorphology and river management**: applications of the River Styles framework. Oxford: Blackwell Publishing, 2013. 416 p.
34. GALBRAITH, R.F., ROBERTS, R.G., LASLETT, G.M., YOSHIDA, H., OLLEY, J.M., 1999. Optical dating of single and multiple grains of quartz from Jinmium rock shelter, northern Australia: Part I, experimental design and statistical models. **Archaeometry** 41, 339–364. https://doi.org/10.1111/j.1475-4754.1999.tb00987.x
35. GARCIA, E. A. **O clima no Pantanal Mato-Grossense**. Corumbá: EMBRAPA-UEPAE Corumbá, 1984. 42 p. (Circular Técnica, 14). Disponível em: http://www.infoteca.cnptia.embrapa.br/infoteca/handle/doc/787712. Acesso em: 15 fev. 2026.
36. GARREAUD, R. D. et al. The Andes climate and weather. **Advances in Geosciences**, v. 22, p. 3-11, 2009. Disponível em: https://adgeo.copernicus.org/articles/22/3/2009/adgeo-22-3-2009.pdf. Acesso em: 15 fev. 2026.
37. GIBLING, M. R. Width and thickness of fluvial channel bodies and valley fills in the geological record: A literature compilation and classification. **Journal of Sedimentary Research**, v. 76, p. 731–770, 2006. DOI: 10.2110/jsr.2006.060
38. HORTON, B.K.; DECELLES, P.G. The modern foreland basin system adjacent to the Central Andes. **Geology**, v.25, n.10, p.895-898, 1997.
39. IRIONDO, M.H.; GARCÍA, N.O. Climatic variations in the Argentine plains during the last 18,000 years. **Palaeogeogr. Palaeoclimatol. Palaeoecol**. v.101, n.3-4, p.209-220, 1993.
40. IRIONDO, M. H.; KRÖHLING, D. M. **Cambios ambientales en la cuenca del río Uruguay**: desde dos millones de años hasta el presente. 1a ed - Santa Fe: Ediciones UNL, 2022. Libro digital, PDF/A.
41. JUNK, W. J.; CUNHA, C. N.; WANTZEN, K. M.; PETERMANN, P.; STRÜSSMANN, C.; MARQUES, M. I.; ADIS, J. Biodiversity and its conservation in the Pantanal of Mato Grosso, Brazil. **Aquatic Science**, v.68, p.278-309, 2006.
42. KUERTEN, S. **Evolução geomorfológica e mudanças ambientais no megaleque do Nabileque, Quaternário do Pantanal Mato-Grossense**. Tese de Doutorado (Geociências e Meio Ambiente) - UNESP, Rio Claro-SP, 2010.
43. KUERTEN, S.; PAROLIN, M.; ASSINE, M.L.; MCGLUE, M.M. Sponge spicules indicate Holocene environmental changes on the Nabileque River floodplain, southern Pantanal, Brazil. **Journal of Paleolimnology**, v.49, n.2, p.171-183, 2013. DOI: 10.1007/s10933-012-9652-z.
44. KUERTEN, S.; STEVAUX, J. C. Megaleques das bacias sedimentares do Chaco e Pantanal: uma revisão comparada. **Revista Brasileira de Geomorfologia**, v. 22, n. 3, p. 567-589, 2021. DOI: 10.20502/rbg.v22i3.1886.
45. LATRUBESSE, E.M.; STEVAUX, J.C.; CREMON, E.H.; MAY, J.; TATUMI, S.H.; HURTADO, M.A.; BEZADA, M.; ARGOLLO, J.B. Late Quaternary megafans, fans and fluvio-aeolian interactions in the bolivian Chaco, Tropical South America. **Palaeogeography, Palaeoclimatology, Palaeoecology**, v.356-357, p.75-88, 2012.
46. LELI, I. T.; STEVAUX, J. C. Origin, evolution, and sedimentary records of islands in large anabranching tropical rivers: The case of the Upper Paraná River, Brazil. **Geomorphology**, v. 358, 107120, 2020. https://doi.org/10.1016/j.geomorph.2020.107120.
47. LEWIN, J.; ASHWORTH, P. J. The negative relief of large river floodplains. **Earth-Science Reviews**, v. 126, p. 194-206, 2014. DOI: 10.1016/j.earscirev.2013.10.014.
48. MACEDO, H. A. **Geomorfologia e hidrossedimentologia da planície do rio Paraguai, da lagoa Vermelha à confluência do rio Miranda, Pantanal Mato-Grossense**. Dissertação de Mestrado (Geociências e Meio Ambiente) – UNESP, Rio Claro-SP, 2013.
49. MACEDO, H.A.; ASSINE, M.L.; SILVA, A.; PUPIM, F.N.; MERINO, E.R.; STEVAUX, J.C. Mudanças paleo-hidrológicas na planície do rio Paraguai, Quaternário do Pantanal. **Revista Brasileira de Geomorfologia**, v.15, n.1, p.75-85, 2014. DOI: 10.20502/rbg.v15i1.431.
50. MACEDO, H.A.; **Evolução geomorfológica e dinâmica hidrossedimentar da planície fluvial Paraguai-Corumbá, Quaternário do Pantanal**. Tese de doutorado (Geociências e Meio ambiente) – UNESP, Rio Claro-SP, 2017.
51. MACEDO, H.A.; STEVAUX, J.C.; SILVA, A.; MERINO, E.R.; LO, E.L.; ASSINE, M.L. Hydrosedimentology of the Paraguay River in the Corumbá fluvial reach, Pantanal wetland. **Revista Brasileira de Geomorfologia**, v. 20, n. 2, p. 255-271, 2019. DOI: 10.20502/rbg.v20i2.1500.
52. MARENGO, J. A.; SAMPAIO, G.; ALVES, L. M. Climate change scenarios in the Pantanal. In: BERGI ER, I.; ASSINE, M. L. (eds.). **Dynamics of the Pantanal wetland in South America**. Cham: Springer, 2015. p. 1-12. DOI: 10.1007/698_2015_357.
53. MARENGO, J. A. et al. Extreme drought in the Brazilian Pantanal in 2019–2020: characterization, causes, and impacts. **Frontiers in Water**, v. 3, artigo 639204, 2021. DOI: 10.3389/frwa.2021.639204.
54. MAY, J. H.; ZECH, R.; VEIT, H. Late Quaternary paleosoil– sediment-sequences and landscape evolution along the Andean piedmont, Bolivian Chaco. **Geomorphology**, v. 98, n. 1-2, p. 34-54, 2008.
55. MCGLUE, M. M.; SILVA, A.; ZANI, H.; CORRADINI, F. A.; PAROLIN, M.; ABEL, E. J.; COHEN, A. S.; ASSINE, M. L.; ELLIS, G. S.; TREES, M. A.; KUERTEN, S.; GRADELLA, F. S.; RASBOLD, G. G. Lacustrine records of Holocene flood pulse

dynamics in the Upper Paraguay River watershed (Pantanal wetlands, Brazil). **Quaternary Research**, v.78, p.285–294, 2012. doi:10.1016/j.yqres.2012.05.015

56. MEIRA, F. C., STEVAUX, J. C., TORRADO, P. V., ASSINE, M. L. Compartimentação e evolução geomorfológica da planície do rio Cuiabá, Pantanal Mato-grossense. **Revista Brasileira de Geomorfologia**, v.20, n.1, (Jan-Mar) p.159-183, 2019. http://dx.doi.org/10.20502/rbg.v20i1.1444
57. MENDES, D. **Geocronologia de formas deposicionais e evolução da planície interleques do Rio Negro, Quaternário da Bacia do Pantanal**. Tese de Doutorado (Geociências e Meio Ambiente) – UNESP, Rio Claro-SP, 2014.
58. MENDES, D.; ASSINE, M.L. Planície interleque do rio Negro, Pantanal Mato-Grossense. In: Congresso da Associação Brasileira de Estudos do Quaternário ABEQUA. 13., 9 a 14 de Outubro de 2011, Armação de Búzios-RJ, Brasil. **Anais...** Rio de Janeiro: ABEQUA, 2013. p.1200-1204. Disponível em: http://www.abequa.org.br/anais_2011.pdf.
59. MERINO, E.R. **Evolução geomorfológica e mudanças paleohidrológicas na porção sul do Pantanal: a planície interleques do rio Negro e leques fluviais coalescentes**. Tese de Doutorado (Geociências e Meio Ambiente) – UNESP, Rio Claro-SP, 2016.
60. MERINO, E.R.; ASSINE, M.L.; PUPIM, F.N. Estilos fluviais e evidências de mudanças ambientais na planície do rio Miranda, Pantanal. **Revista Brasileira de Geomorfologia**, v.14, n.2, p.127–134, 2013.
61. METCALFE, S.E.; WHITNEY, B.S.; FITZPATRICK, K.A.; MAYLE, F.E.; LOADER, N.J.; STREET-PERROTT, F.A.; MANN, D.G. Hydrology and climatology at Laguna La Gaiba, lowland Bolivia: complex responses to climatic forcings over the last 25 000 years. **Journal of Quaternary Science**, v.29, n.3, p.289-300, 2014. DOI: 10.1002/jqs.2702
62. MIALL, A. D. Fluvial Sedimentology. Calgary, Alberta, Canada: **Canadian Society of Petroleum Geologists**, v.5, 1978, 859p.
63. MOSBLECH, N.A.S.; BUSH, M.B.; GOSLING, W.D.; HODELL, D.; THOMAS, L.; VAN CALSTEREN, P.; CORREA-METRIO, A.; VALENCIA, B.G.; CURTIS, J.; VAN WOESIK, R.. North Atlantic forcing of Amazonian precipitation during the last ice age**. Nat. Geosci**., v.5, p.817-820, 2012. DOI: 10.1038/ngeo1588.
64. MURRAY, A.S.; WINTLE, A.G. Luminescence dating of quartz using an improved single-aliquot regenerative-dose protocol. **Radiation Measurements**, v.32, p.57-73, 2000. PII: S13 5 0- 44 8 7(99)0 02 5 3-X.
65. NEIFF, Juan José. Diversity in some tropical wetland systems of South America. In: GOPAL, B.; JUNK, W. J.; DAVIS, J. A. (Ed.). **Biodiversity in wetlands: assessment, function and conservation**. Leiden: Backhuys Publishers, 2001. p. 157-186.
66. NOVELLO, V.F.; CRUZ, F.W.; VUILLE, M.; STRÍKIS, N.M.; EDWARDS LAWRENCE, R.; CHENG, H.; EMERICK, S.; DE PAULA, M.S.; LI, X.; BARRETO, E.S.; KARMANN, I.; SANTOS, R.V. A high-resolution history of the South American Monsoon from Last Glacial Maximum to the Holocene. **Scientific Reports**, v.7, n.44267, 2017. DOI: 10.1038/srep44267.
67. PARANHOS FILHO, A.C.; NUMMER, A.R.; ALBREZ, E.A.; RIBEIRO, A.A.; MACHADO, R. A study of structural lineaments in Pantanal (Brazil) using remote sensing data. **An Acad Bras Cienc**. v.85, n.3, p. 913-922. 2013. Doi: 10.1590/S0001-37652013000300007.
68. POR, F.D. **The Pantanal of Mato Grosso (Brazil)** - World's Largest Wetlands. Dordrecht, The Netherland: Kluvwer Academic Publishers,1995, 122p.
69. PUPIM, F.N. **Geomorfologia e paleo-hidrologia dos megaleques dos rios Cuiabá e São Lourenço, Quaternário da Bacia do Pantanal**. Tese de Doutorado (Geociências e Meio Ambiente) - UNESP, Rio Claro-SP, 2014, 109p.
70. PUPIM, F.N.; ASSINE, M.L.; MERINO, E.R.; MACEDO, H.A.; SILVA, A. A planície interleques do rio Piquiri, bacia do Pantanal. In: Simpósio de Geotecnologias no Pantanal – GEOPANTANAL, 5. 22 a 26 de novembro 2014, Campo Grande, MS. **Anais...** São José dos Campos, SP: INPE, 2014. p.848-857. CD rom.
71. PUPIM, F.N.; ASSINE, M.L.; SAWAKUCHI, A.O. Late Quaternary Cuiabá megafan, Brazilian Pantanal: Channel patterns and paleoenvironmental changes. **Quaternary International**, v.438, Parte A, p.108-125, 2017. DOI: 10.1016/j.quaint.2017.01.013.
72. RASBOLD, G.G.; MCGLUE, M.M.; STEVAUX, J.C.; PAROLIN, M.; SILVA, A.; BERGIE, I. Sponge spicule and phytolith evidence for Late Quaternary environmental changes in the tropical Pantanal wetlands of western Brazil. **Palaeogeography, Palaeoclimatology, Palaeoecology**, v. 518, p. 119–133, 2019. DOI: 10.1016/j.palaeo.2019.01.015.
73. RASBOLD, G.G.; MCGLUE, M.M.; STEVAUX, J.C., PAROLIN, M.M.; SILVA, A.; BERGIER, I. Enhanced middle Holocene organic carbon burial in tropical floodplain lakes of the Pantanal (South America). **Journal of Paleolimnology**, DOI 10.1007/s10933-020-00159-5; 2020.
74. REBOUÇAS, A.; BRAGA, B.; TUNDISI, J. G. (organizadores). **Águas doces no Brasil**: capital ecológico, uso e conservação. São Paulo: Escrituras Editora, 2002.
75. REIMER, P. J. et al. The IntCal20 Northern Hemisphere radiocarbon age calibration curve (0–55 cal kBP). **Radiocarbon**, v. 62, n. 4, p. 725-757, 2020. DOI: 10.1017/RDC.2020.41.

76. SAWAKUCHI, A.O.; KALCHGRUBER, R.; GIANNINI, P.C.F.; NASCIMENTO Jr., D.R.; GUEDES, C.C.F.; UMISEDO, N.K. The development of blowouts and foredunes in the Ilha Comprida barrier (Southeastern Brazil): the influence of Late Holocene climate changes on coastal sedimentation. **Quaternary Science Reviews**, v.27, p.2076-2090, 2008.
77. SILVA, **A. Geomorfologia do megaleque do rio Paraguai, Quaternário do Pantanal Mato-Grossense, Centro-Oeste do Brasil.** Tese de Doutorado (Geociências e Meio Ambiente) - UNESP, Rio Claro-SP, 2010.
78. SOUZA, C. A. **Dinâmica do corredor fluvial do rio Paraguai entre a cidade de Cáceres e a estação ecológica da ilha de Taiamã - MT**. Tese de Doutorado – UFRJ, Rio de Janeiro-RJ, 2004.
79. STEVAUX, J.C. The Upper Paraná River (Brazil): Geomorphology, sedimentology and paleoclimatology. **Quaternary International**, 21:143-161, 1994.
80. STEVAUX, J.C. Climatic events during the Late Pleistocene and Holocene in the Upper Parana River: Correlation with NE Argentina and South-Central Brazil. **Quaternary International**, v. 72, p. 73-86, 2000.
81. STEVAUX, J.C.; MACEDO, H.A., ASSINE, M.L., SILVA, A. Changing fluvial styles and backwater flooding along the UpperParaguay River plains in the Brazilian Pantanal wetland . **Geomorphology**, n. 350, 106906. 2020.
82. THALMEIER, M. B.; KRÖHLING, D. M.; BRUNETTO, E. The geomorphology and Late Quaternary sedimentary record of the Salado/Juramento fluvial megafan, Central Andes foreland basin (Chaco Plain, Argentina). **Geomorphology**, n. 373, 107495, 2021. doi: 10.1016/j.geomorph.2020.107495.
83. TRENHAILE, A. S. **Geomorphology**: A Canadian Perspective. Oxford University Press. 2016
84. USSAMI, N.; SHIRAIWA, S.; DOMINGUEZ, J.M.L. Basement reactivation in a sub-Andean foreland flexural bulge: Pantanal wetland, SW Brazil. **Tectonics**, v.18 n.1, p.25-39, 1999.
85. WANG, X.; EDWARDS, R. L.; AULER, A. S.; CHENG, H.; KONG, X.; WANG, Y.; CRUZ, F. W.; DORALE, J. A.; CHIANG, H-W. Hydroclimate changes across the Amazon lowlands over the past 45,000 years. **Nature Letter Research**, v.541, p.204-219, 2017. doi:10.1038/nature20787.
86. WHITNEY, B. S.; MAYLE, F. E.; PUNYASENA, S. W.; FITZPATRICK, K. A.; BURN, M. J.; GUILLEN, R.; CHAVEZ, E.; MANN, D.; PENNINGTON, R. T.; METCALFE, S. E.. A 45 kyr palaeoclimate record from the lowland interior of tropical South America. **Palaeogeography, Palaeoclimatology, Palaeoecology**, v.307, p.177-192, 2011. doi:10.1016/j.palaeo.2011.05.012
87. WILLIAMS, G. P. Paleofluvial estimates from dimensions of former channels and meanders. In: **Flood Geomorphology**, New York: John Wiley & Sons, 1988, p. 321-334.
88. WINTLE, A.G.; MURRAY, A.S. A review of quartz optically stimulated luminescence characteristics and their relevance in single-aliquot regeneration dating protocols. **Radiation Measurements**, v.41, p.369-391, 2006. doi:10.1016/j.radmeas.2005.11.001
89. ZANI, H. **Mudanças morfológicas na evolução do megaleque do Taquari: uma análise baseada em dados orbitais**. Dissertação de Mestrado (Geociências e Meio Ambiente) - Instituto de Geociências e Ciências Exatas, UNESP, Rio Claro-SP, 2008, 85p.
90. ZANI, H.; ASSINE, M.L.; SILVA, A.; CORRADINI, F.A. Redes de drenagem distributárias e formas deposicionais no megaleque do Taquari, Pantanal Mato-Grossense: Uma análise baseada no processamento de dados SRTM. **Revista Brasileira de Geomorfologia**, v.10, p.23-28, 2009.
91. ZANI, H.; ASSINE, M.L.; McGLUE, M.M. Remote sensing analysis of depositional landforms in alluvial settings: Method development and application to the Taquari megafan, Pantanal (Brazil). **Geomorphology**, v.161-162, p.82-92, 2012. DOI: 10.1016/j.geomorph.2012.04.003.